AMERICAN SOCIETY FOR MICROBIOLOGY | Journal of Virology®

PATHOGENESIS AND IMMUNITY

Influenza Virus Infection Enhances Antibody-Mediated NK Cell Functions via Type I Interferon-Dependent Pathways

Sinthujan Jegaskanda,[a] Hillary A. Vanderven,[a,b] Hyon-Xhi Tan,[a] Sheilajen Alcantara,[a] Kathleen M. Wragg,[a] Matthew S. Parsons,[a] Amy W. Chung,[a] Jennifer A. Juno,[a] Stephen J. Kent[a,c,d]

[a]Department of Microbiology and Immunology, University of Melbourne, at the Peter Doherty Institute for Infection and Immunity, Melbourne, Victoria, Australia
[b]Biomedicine, College of Public Health, Medical and Veterinary Sciences, James Cook University, Douglas, Queensland, Australia
[c]ARC Centre of Excellence in Convergent Bio-Nano Science and Technology, The University of Melbourne, Melbourne, Victoria, Australia
[d]Melbourne Sexual Health Centre, Alfred Hospital, Monash University Central Clinical School, Melbourne, Victoria, Australia

ABSTRACT Natural killer (NK) cells are an important component in the control of influenza virus infection, acting to both clear virus-infected cells and release antiviral cytokines. Engagement of CD16 on NK cells by antibody-coated influenza virus-infected cells results in antibody-dependent cellular cytotoxicity (ADCC). Increasing the potency of antibody-mediated NK cell activity could ultimately lead to improved control of influenza virus infection. To understand if NK cells can be functionally enhanced following exposure to influenza virus-infected cells, we cocultured human peripheral blood mononuclear cells (PBMCs) with influenza virus-infected human alveolar epithelial (A549) cells and evaluated the capacity of NK cells to mediate antibody-dependent functions. Preincubation of PBMCs with influenza virus-infected cells markedly enhanced the ability of NK cells to respond to immune complexes containing hemagglutinin (HA) and anti-HA antibodies or transformed allogeneic cells in the presence or absence of a therapeutic monoclonal antibody. Cytokine multiplex, RNA sequencing, supernatant transfer, Transwell, and cytokine-blocking/cytokine supplementation experiments showed that type I interferons released from PBMCs were primarily responsible for the influenza virus-induced enhancement of antibody-mediated NK cell functions. Importantly, the influenza virus-mediated increase in antibody-dependent NK cell functionality was mimicked by the type I interferon agonist poly(I·C). We conclude that the type I interferon secretion induced by influenza virus infection enhances the capacity of NK cells to mediate ADCC and that this pathway could be manipulated to alter the potency of anti-influenza virus therapies and vaccines.

IMPORTANCE Protection from severe influenza may be assisted by antibodies that engage NK cells to kill infected cells through ADCC. Studies have primarily focused on antibodies that have ADCC activity, rather than the capacity of NK cells to become activated and mediate ADCC during an influenza virus infection. We found that type I interferon released in response to influenza virus infection primes NK cells to become highly reactive to anti-influenza virus ADCC antibodies. Enhancing the capacity of NK cells to mediate ADCC could assist in controlling influenza virus infections.

KEYWORDS ADCC, influenza, NK cell, interferons

Natural killer (NK) cells may play a key role in limiting influenza virus infection by eliminating influenza virus-infected cells and releasing antiviral cytokines. NK cells mediate the lysis of influenza virus-infected cells by direct cytotoxicity and antibody-dependent cellular cytotoxicity (ADCC). Activating receptors on NK cells, including NKp46 and NKp44, bind to the viral glycoprotein hemagglutinin (HA) expressed on the

Citation Jegaskanda S, Vanderven HA, Tan H-X, Alcantara S, Wragg KM, Parsons MS, Chung AW, Juno JA, Kent SJ. 2019. Influenza virus infection enhances antibody-mediated NK cell functions via type I interferon-dependent pathways. J Virol 93:e02090-18. https://doi.org/10.1128/JVI.02090-18.

Editor Stacey Schultz-Cherry, St. Jude Children's Research Hospital

Address correspondence to Sinthujan Jegaskanda, sjeg@unimelb.edu.au, or Stephen J. Kent, skent@unimelb.edu.au.

Received 26 November 2018
Accepted 29 November 2018
Accepted manuscript posted online 12 December 2018
Published 19 February 2019

surface of influenza virus-infected cells (1, 2). Direct interactions between NK cell-activating receptors and influenza HA can lead to the release of cytolytic granules and proinflammatory cytokines from activated NK cells (3, 4). The primary receptor responsible for NK cell-mediated ADCC in humans is the low-affinity Fc gamma receptor FcγRIIIa (CD16), which, upon binding IgG (mainly IgG1 and/or IgG3), may result in NK cell activation (5–8). Activated NK cells release cytokines with potent antiviral activity, such as interferon gamma (IFN-γ) and tumor necrosis factor (TNF), as well as cytotoxic granules containing perforin and granzyme B. NK cell degranulation kills influenza virus-infected target cells, and cytokine secretion promotes an antiviral microenvironment aiding in the control of influenza virus infection.

In recent years, influenza virus research has focused heavily on the induction and therapeutic potential of broadly neutralizing antibodies (bNAbs) targeting HA. HA stem-specific bNAbs, like CR9114, have potent ADCC activity and protect mice from influenza virus infection in an Fc receptor-dependent manner (9–14). He et al. recently showed that the depletion of alveolar macrophages (AMs), but not NK cells, reduced the protective capacity of HA stem-specific bNAbs in a murine model of influenza virus infection (15). It is unclear whether AM-mediated protection in mice is the result of ADCC and/or antibody-dependent phagocytosis (ADP), but human and murine Fc receptors differ significantly both in affinity and in cellular distribution (5). Furthermore, it was demonstrated that an HA stem-specific monoclonal antibody (MAb) can provide robust protection from experimental human influenza virus challenge (16). Given the increased interest in HA MAbs with ADCC activity (17–19), it is important to understand the mechanisms that influence influenza virus-specific ADCC. Prior studies performed with other viruses (HIV-1, reoviruses, etc.) and cancer immunotherapies have shown that antibody-dependent NK cell responses can be enhanced by coreceptor engagement (20, 21), Fc receptor polymorphisms (14), modification of antibody glycosylation (22), addition of Toll-like receptor (TLR) agonists (23), and the cytokine milieu, including type I interferon (IFN) secretion (24). However, the impact of influenza virus infection on NK cell ADCC activity has not been thoroughly investigated.

A major role of the influenza virus nonstructural 1 (NS1) protein is to antagonize the induction of a type I IFN response, but circulating strains of human influenza virus differ significantly in their ability to block the transcription of type I IFN. Seasonal strains of H3N2 and H2N2 influenza virus cannot block the induction of a type I IFN-β response *in vitro*. However, A/Puerto/Rico/1934 (H1N1) (PR8) and H1N1 2009 pandemic (H1N1pdm09) strains of influenza virus express NS1 proteins that can inhibit activation of IFN-responsive factor 3 (IRF3) and block transcription of IFN-β (25). In the late 1970s, Santoli et al. showed that the type I IFN induced by infection with A/Hong Kong/107/1968 (H3N2) influenza virus enhanced the cytotoxic capacity of peripheral blood lymphocytes (PBLs) *in vitro* (26). Direct infection of PBLs with influenza virus as well as coculture with influenza virus-infected fibroblasts led to a dramatic increase in the cytotoxic capacity of PBLs, as measured by direct (or antibody-independent) cytolysis of influenza virus-infected and uninfected target cells (26). Gerosa et al. later demonstrated that the cytolytic activity of human NK cells against uninfected Daudi cells was markedly increased by type I IFN secretion from plasmacytoid dendritic cells (pDCs) in response to inactivated influenza virus (27). These studies highlight the importance of type I IFN in stimulating human NK cell functionality, but the effect that influenza virus infection can have on antibody-mediated NK cell functions has not been addressed to date.

To assess the impact of influenza virus infections on antibody-mediated NK cell responses, we developed a coculture method incubating human peripheral blood mononuclear cells (PBMCs) with infected respiratory epithelial cells. Following incubation with influenza virus-infected cells, PBMCs were removed from coculture, washed, and incubated (i.e., rested) for a period without virus-infected cells. The NK cells were then tested for degranulation and cytokine release in response to a variety of antibody-mediated stimuli. Through extensive cytokine profiling and transcriptional and flow cytometry analyses, we show that influenza virus infection potently and durably

enhances antibody-dependent NK cell responses via type I IFN release from PBMCs. Our work suggests that avenues to manipulate antibody-dependent NK cell functions should be assessed for the improved control of influenza virus infection.

RESULTS

Exposure to influenza virus-infected cells enhances antibody-mediated NK cell functionality. Previous studies have shown that influenza virus-exposed NK cells demonstrate an increased capacity to become activated and mediate direct cytolysis of target cells (26, 27). We hypothesized that the antibody-dependent functions of NK cells may also be enhanced following exposure to influenza virus-infected cells. To study this in detail, we established an *in vitro* primary human cell model wherein PBMCs were cocultured with either influenza virus-infected or uninfected respiratory epithelial cells, removed from coculture, washed, rested, and evaluated for antibody-mediated NK cell responses (Fig. 1A). Using this coculture method, we first studied the ability of NK cells to become activated in response to engagement of their Fc receptor (FcγRIIIa) by anti-CD16 antibody, HA-specific antibodies (in plate-bound immune complexes), and a therapeutic MAb targeting transformed cell lines. NK cells ($CD3^-$ $CD56^+$) were assessed for activation by measuring the surface degranulation marker CD107a (LAMP-1) and intracellular expression of IFN-γ by flow cytometry (Fig. 1A).

We found that influenza virus-exposed PBMCs had a substantially higher frequency of activated NK cells expressing both CD107a and IFN-γ upon CD16 cross-linking (by plate-bound anti-CD16 antibody) than influenza virus-unexposed PBMCs (Fig. 1A). This finding was consistent across PBMCs from 12 human PBMC donors, with higher frequencies of total $CD107a^+$ NK cells (Fig. 1B; mean frequency, 54.6% in influenza virus-exposed PBMCs versus 7.8% in influenza virus-unexposed PBMCs) and $CD107a^+$ IFN-γ-positive (IFN-γ^+) NK cells (Fig. 1C; mean frequency, 37.7% in influenza virus-exposed PBMCs versus 1.5% in influenza virus-unexposed PBMCs) being observed in influenza virus-exposed PBMCs. A prolonged resting period following influenza virus exposure did not abrogate the enhanced functionality of influenza virus-exposed NK cells, with PBMCs rested for up to 96 h postexposure still showing elevated frequencies of activated NK cells compared to influenza virus-unexposed PBMCs (Fig. 1D and E; $P < 0.05$ for influenza virus-exposed versus influenza virus-unexposed PBMCs for 12-, 24-, 48-, and 96-h resting periods). The resting period was not extended further, as fewer cells were recovered from these primary NK cells in culture beyond 96 h. Analysis of an additional proinflammatory cytokine, TNF, showed NK cell activation similar to that observed for CD107a and IFN-γ (see Fig. S1 in the supplemental material). Thus, influenza virus exposure consistently leads to more functional NK cells (across all three activation markers) through CD16 engagement.

Anti-CD16 antibodies mimic the process by which the Fc portion of antibodies engages CD16 (FcγRIIIa) receptors to trigger ADCC. To directly assess antibody-mediated NK cell activation against influenza virus proteins, we incubated influenza virus-exposed and -unexposed PBMCs on plates coated with the influenza virus HA protein and HA-specific antibodies from pooled human intravenous immunoglobulin (IVIG). Influenza virus-unexposed PBMCs had low HA-specific antibody-dependent NK cell activation, as measured by total $CD107a^+$ NK cells (mean frequency at 12-h time point, 3.4%) and $CD107a^+$ IFN-γ^+ NK cells (mean frequency at 12-h time point, 1.0%) (Fig. 2A). However, NK cells in influenza virus-exposed PBMCs had greater than 9-fold higher mean frequencies of total CD107a expression (mean frequency at 12-h time point, 33.2%) and coexpression of CD107a and IFN-γ (mean frequency at 12-h time point, 20.0%) (Fig. 2B and C). As expected, influenza virus-exposed NK cells had much lower activation in the absence of influenza virus-specific antibodies (naive plasma control), similar to controls, where there was no antibody present (phosphate-buffered saline [PBS] control or plates coated with the HIV gp140 protein, to which there are no antibodies in IVIG; Fig. 2). Again, this effect was consistent across multiple PBMC donors and was present even after longer periods of resting following influenza virus exposure

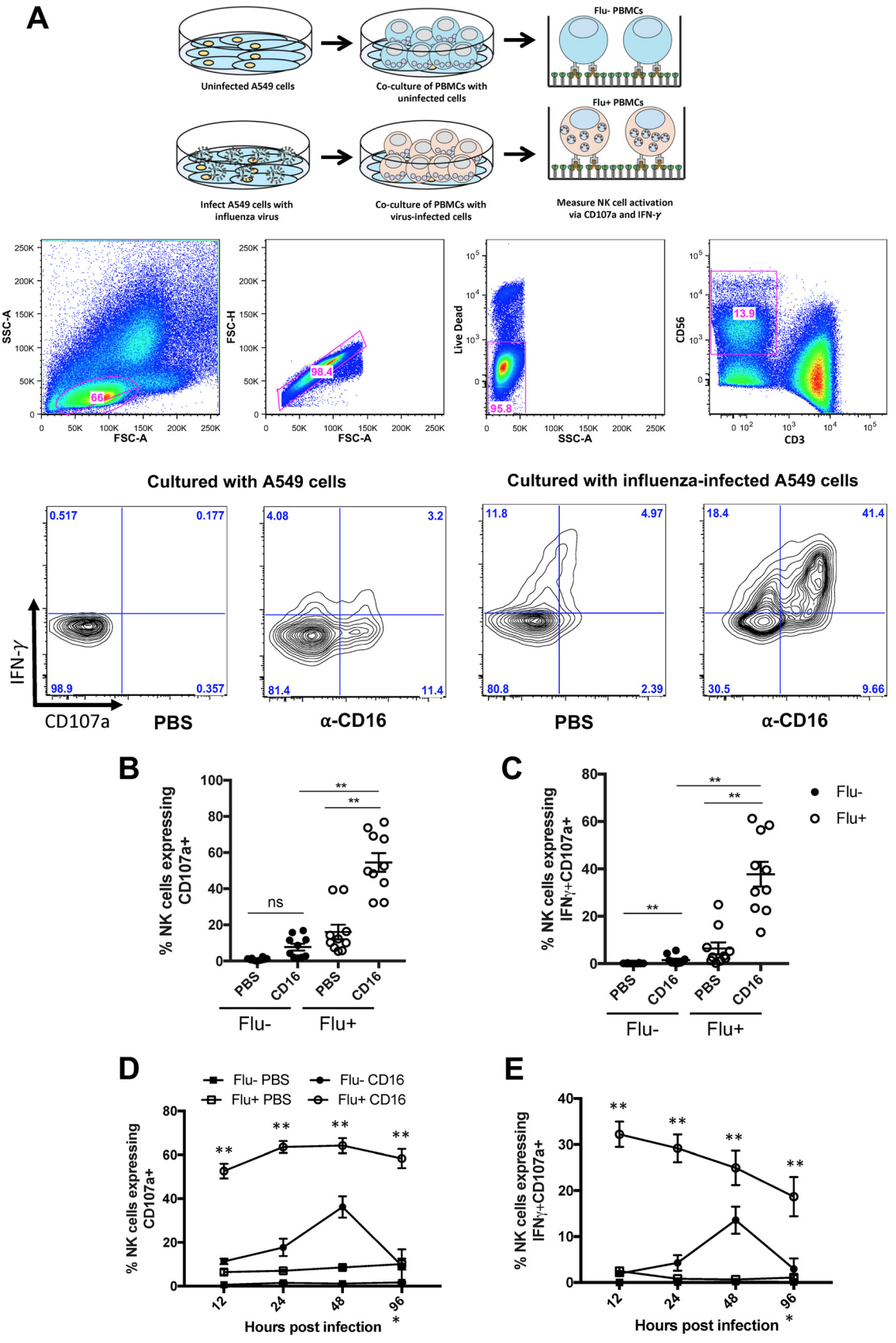

FIG 1 Prior exposure to influenza virus-infected cells induces higher activation of NK cells upon CD16 cross-linking. (A) PBMCs were exposed to influenza virus-infected cells *in vitro* and measured for their CD16-mediated activation potential. Healthy donor PBMCs

(Continued on next page)

(Fig. 2). These data show that influenza virus infection results in enhanced activation of NK cells via influenza virus-specific antibodies.

NK cell activation induced by plate-bound antigen-antibody complexes does not necessarily reflect stimulation by whole-cell targets. We therefore tested whether influenza virus exposure increases direct and antibody-dependent NK cell activation in the presence of transformed cell lines. The combined expression of ligands for activating receptors and a lack of major histocompatibility complex (MHC) class I expression on K562 cells result in NK cell activation. In response to K562 cells, NK cell activation was consistently higher among influenza virus-exposed NK cells than influenza virus-unexposed NK cells (at a 1:1 effector-to-target cell [E:T] ratio, the mean frequency of CD107a$^+$ NK cells was 20.9% versus 1.5%, respectively, and the mean frequency of CD107a$^+$ IFN-γ^+ NK cells was 15.9% versus 0.3%, respectively; Fig. 3A and B). To extend this observation to antibody-dependent NK cell activation, we measured activation of influenza virus-exposed (and influenza virus-unexposed) NK cells in the presence of an HLA-I-devoid 721.221 B cell line with or without the anti-CD20 antibody rituximab. Our group has previously shown that NK cells can become activated by exposure to 721.221 cells alone, as well as following the addition of rituximab (28). Influenza virus-exposed PBMCs exhibited greater NK cell activation than unexposed PBMCs following stimulation with 721.221 cells alone (Fig. 3C and D) or 721.221 cells plus rituximab (Fig. 3E and 3F). Antibody-dependent NK cell activation was consistently higher for influenza virus-exposed NK cells than influenza virus-unexposed NK cells across all E:T ratios tested (Fig. 3D). Further, influenza virus-exposed NK cells isolated from three PBMC donors demonstrated an increase in cytotoxicity against 721.221 cells relative to influenza virus-unexposed NK cells using a nonradioactive lactate dehydrogenase (LDH) cytotoxicity assay (Fig. 3G). These experiments corroborate our prior results showing that influenza virus exposure increases the capacity of NK cells to become activated by both direct and antibody-dependent mechanisms.

Phenotypic changes in NK cells following influenza virus exposure. The enhanced capacity of NK cells to become activated following influenza virus exposure may be reflected in transcriptional and/or phenotypic changes in the NK cells. To probe for differential transcriptional patterns between influenza virus-exposed and -unexposed NK cells, PBMCs from three separate donors were first incubated with either infected or uninfected A549 cells. After resting, the NK cells were directly sorted from whole PBMCs for downstream RNA isolation and transcriptional profiling. The top 100 genes with a log fold change (log FC) of greater than 2 or less than -2 and significant differential expression ($P < 0.05$) (listed in Table S1) displayed distinct clustering of influenza virus-exposed and influenza virus-unexposed NK cells (Fig. 4A). The top upregulated genes ($P < 0.05$, log FC > 2) were gathered, and clustered pathway analysis was performed to determine common pathways used by influenza virus-exposed NK cells (Fig. 4B). Cytokine and interferon signaling pathways were overrepresented in influenza virus-exposed NK cells, indicating that secreted factors influence NK cell activation. These data suggest the involvement of type I IFN pathways, as numerous type I IFN-stimulated genes (Mx1, IFN-γ, IFIH1/MDA-5, DDX58/RIG-I, and multiple GBPs) and

FIG 1 Legend (Continued)
($n = 10$ donors) were incubated with a confluent monolayer of uninfected or PR8-infected alveolar epithelial (A549) cells for 12 h at 37°C. Donor PBMCs were then removed, washed, and cultured (i.e., rested) in complete medium for at least 12 h at 37°C in the absence of influenza virus-infected or uninfected A549 cells. To measure CD16-mediated activation potential, NK cells were incubated with plate-bound anti-CD16 antibody and assessed for activation by IFN-γ and CD107a expression via flow cytometry. Samples were analyzed by gating on lymphocytes, single cells, Aqua LIVE/DEAD-negative cells, and CD3$^-$ CD56$^+$ NK cells. Representative plots of CD3$^-$ CD56$^+$ NK cells expressing IFN-γ and CD107a from PBMCs that were exposed to PR8-infected or uninfected A549 cells are shown. SSC-A, side scatter area; FSC-A; forward scatter area; FSC-H, forward scatter height. (B and C) The frequency of CD3$^-$ CD56$^+$ NK cells expressing CD107a alone (B) or CD107a and IFN-γ (C) was examined for influenza virus-exposed (Flu$^+$; open circles) and influenza virus-unexposed (Flu$^-$; solid circles) PBMCs. (D and E) Following exposure to influenza virus-infected cells (open symbols) or uninfected cells (solid symbols), donor PBMCs ($n = 10$ donors; *, $n = 5$ donors) were rested for either 12, 24, 48, or 96 h and subsequently assessed for the frequency of NK cells expressing CD107a alone (D) or CD107a and IFN-γ (E) following CD16 cross-linking. Groups were analyzed via one-way ANOVA with Sidak's multiple-comparison test. **, $P < 0.005$; ns, not significant. Bars represent mean values with SEM.

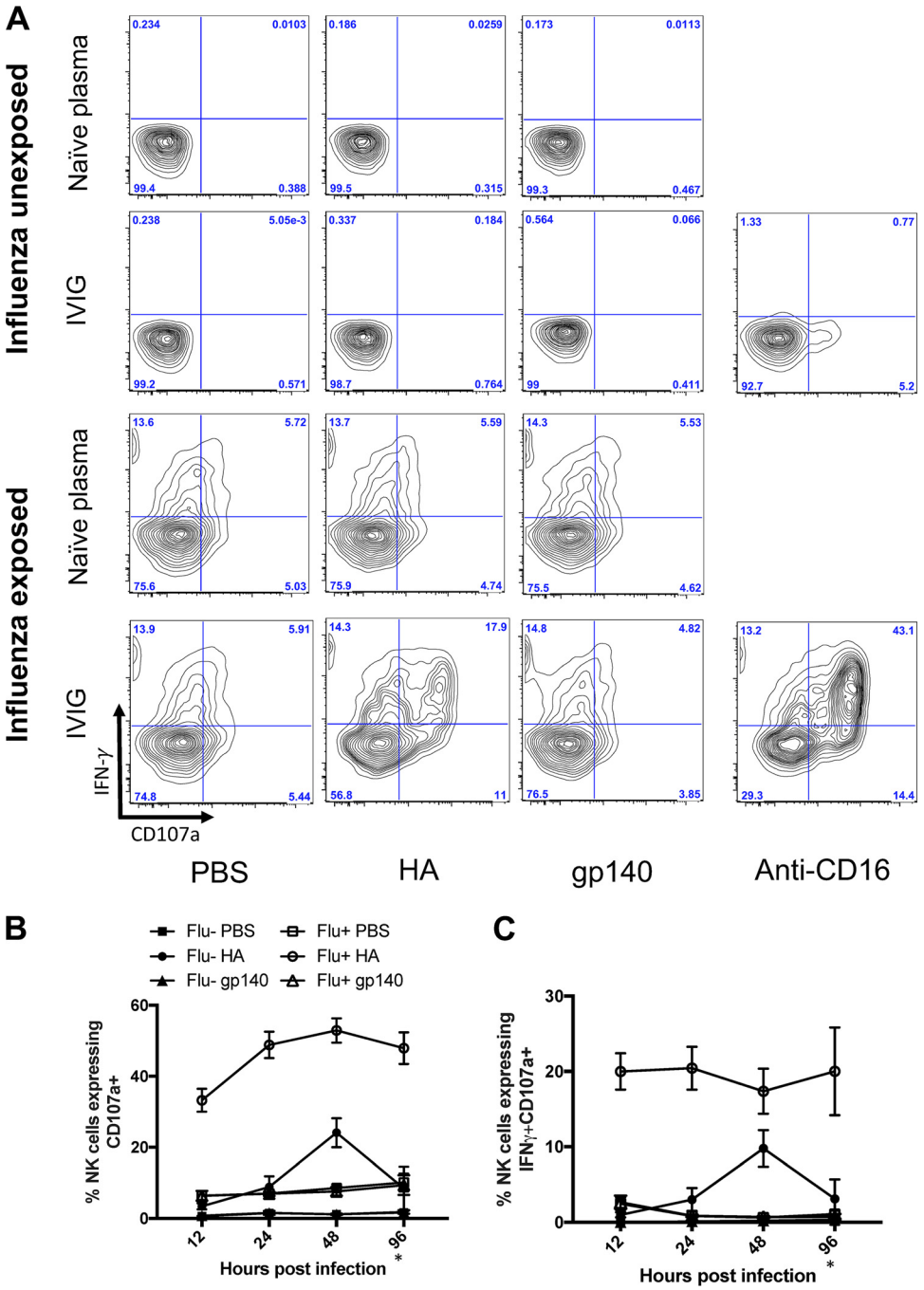

FIG 2 Prior exposure to influenza virus-infected cells induces greater NK cell activation in the presence of HA-IgG immune complexes. (A) Representative plots show the activation of NK cells in PBMCs, which were exposed to either uninfected A549 cells or influenza virus-infected A549 cells, as described in the legend to Fig. 1. NK cell activation was tested following incubation of PBMCs with plate-bound anti-CD16 antibody or plate-bound recombinant PR8 protein, HIV gp140, or PBS in the presence of IVIG (10 μg/ml) or naive macaque serum. NK cell activation was assessed by IFN-γ and CD107a expression using flow cytometry. (B, C) Healthy donor PBMCs (n = 10 donors; *, n = 5 donors) were rested for either 12, 24, 48, or 96 h after exposure to influenza virus-infected (open symbols) or uninfected (solid symbols) cells. NK cell activation was assessed by the frequency of NK cells expressing CD107a alone (B) or CD107a and IFN-γ (C) following incubation with IVIG and PBS (squares), IVIG and recombinant HA (circles), or IVIG and HIV gp140 (triangles).

transcription factors (STAT1, STAT2, and IRF8) were upregulated in influenza virus-exposed NK cells. Surface markers of activation, such as lymphocyte activating gene 3 (LAG-3) and CD69, were also significantly upregulated at the transcriptional level following NK cell exposure to influenza virus-infected cells.

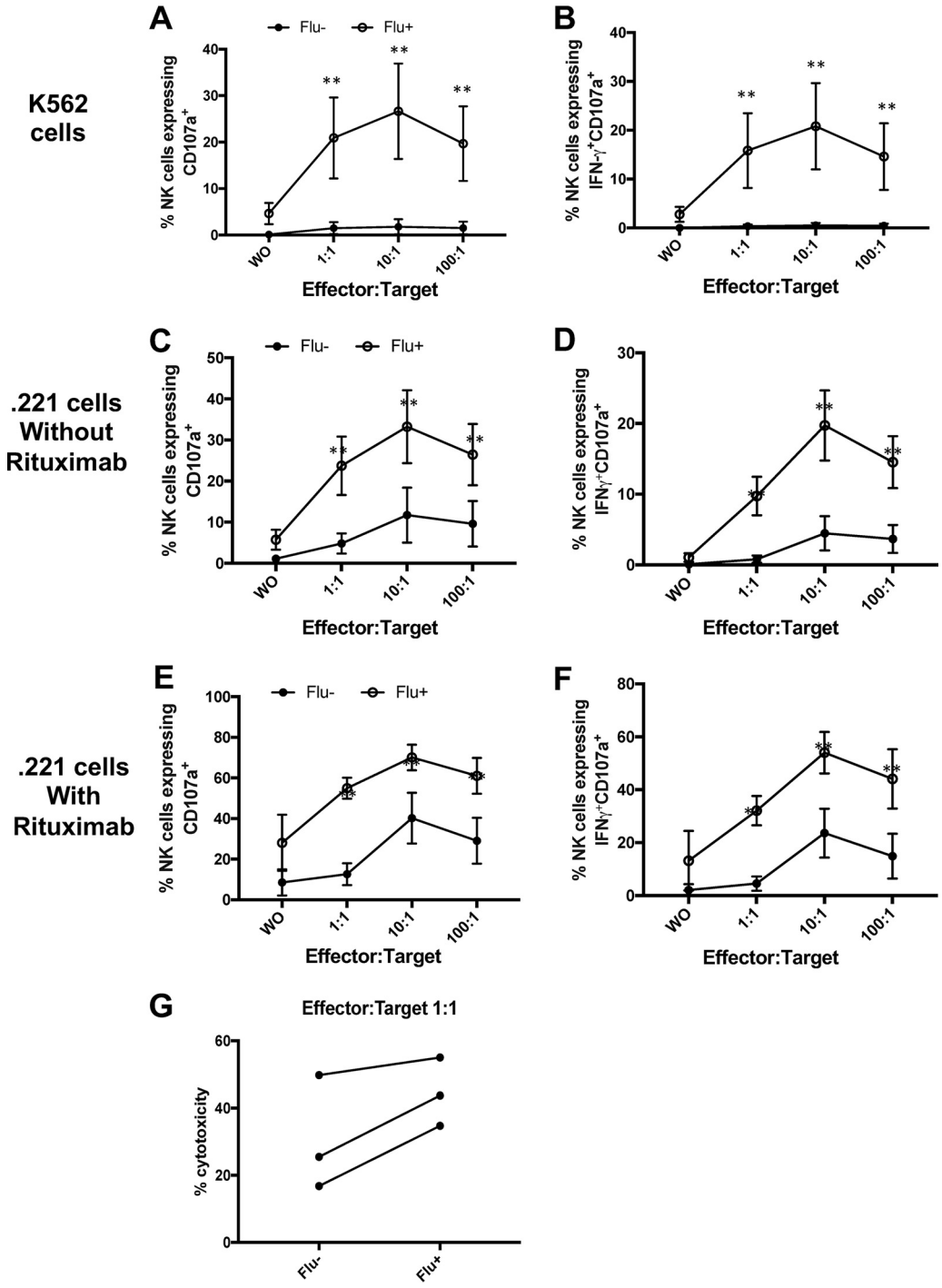

FIG 3 Prior exposure to influenza virus-infected cells induces higher direct and antibody-mediated NK cell activation against tumor cell lines. (A to D) To measure direct activation, NK cells in influenza virus-exposed (open symbols) or -unexposed (solid symbols) PBMCs were tested for activation following incubation alone (without virus [WO]), with K562 cells (A, B), or with 722.221 cells (C, D) at effector-to-target cell (E:T) ratios of 1:1, 10:1, and 100:1. (E, F) To measure the ADCC potential, NK cells in influenza virus-exposed (open symbols) or -unexposed (solid symbols) PBMCs were tested for activation following incubation with rituximab (10 μg/ml) alone (without virus) or with rituximab and 722.221 cells at E:T ratios of 1:1, 10:1, and 100:1. NK cell activation was then assessed by expression of CD107a alone (A, C, E) or CD107a and IFN-γ (B, D, F) using flow cytometry. (G) To measure target cell killing, NK cells were isolated from influenza virus-exposed or -unexposed PBMCs and cocultured with 721.221 target cells at effector-to-target cell ratios of 1:1. After 4 h, LDH release was measured and the percent cytotoxicity was normalized to spontaneous effector-and-target cell values and maximum target cell LDH release. Groups were analyzed via one-way ANOVA with Sidak's multiple-comparison test. **, $P < 0.05$. Bars represent mean values with SEM.

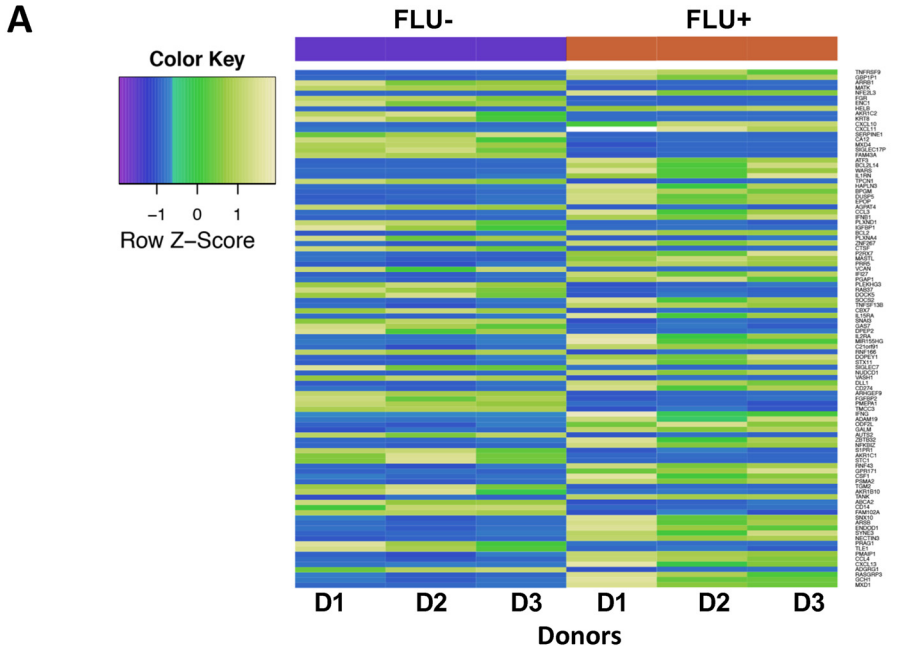

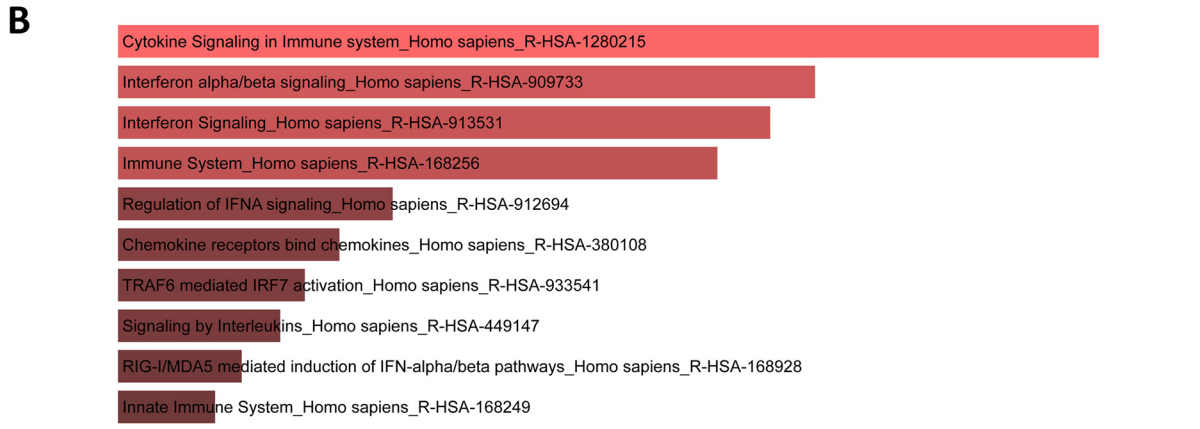

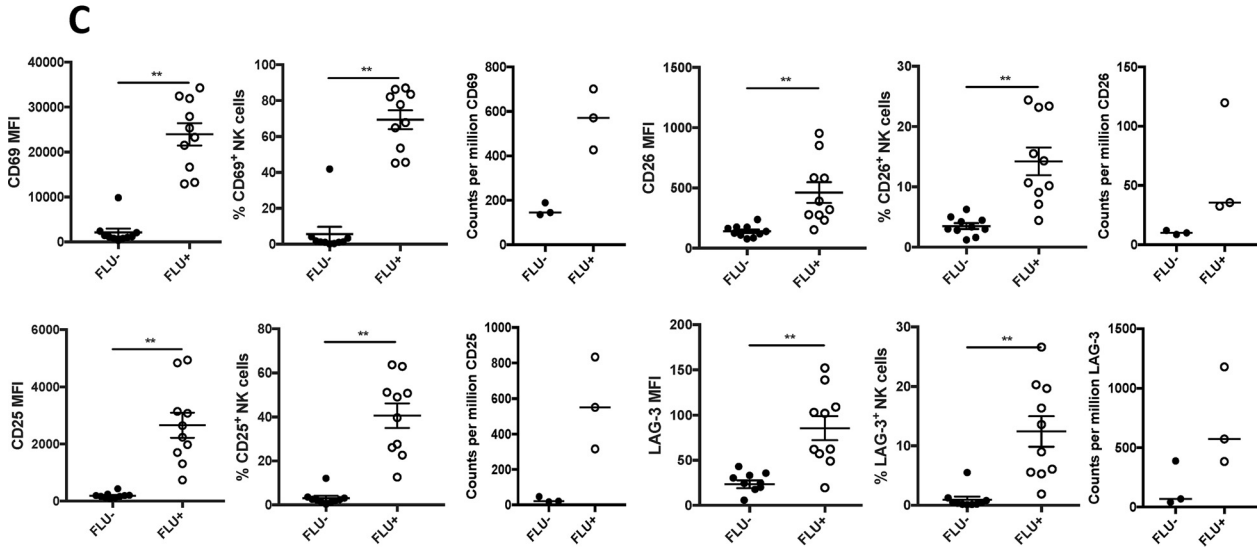

FIG 4 Gene expression profiles and phenotypic markers of influenza virus-exposed NK cells. NK cells (live, $CD3^-$ $CD56^+$) were sorted from donor PBMCs ($n = 3$ donors) after exposure to infected or uninfected A549 cells. Sorted NK cells were then tested for differential gene expression by RNA sequencing. (A) Transcriptional profile based on the top 100 differentially expressed genes of sorted NK cells previously exposed to infected or

(Continued on next page)

To complement and confirm the RNA sequencing (RNAseq) results, we measured the expression of a variety of surface and intracellular markers in influenza virus-exposed and -unexposed NK cells by flow cytometry. NK cells were assessed for changes in protein expression and the frequency of cells with surface activating receptors (CD16, NKG2C, NKG2D, NKp30, NKp44, and NKp46), inhibitory receptors (NKG2A, CD158, and CD158e), differentiation markers (CD57), activation markers (Ki-67, CD25, CD69, granzyme B, LAG-3, CD26, and CD62L), and transcription factors (T-bet, PLZF, and Eomes). We observed no significant difference in the frequency or mean fluorescence intensity of some common NK cell receptors and markers, including activating receptors (CD16, NKp46, NKG2C, and NKG2D), inhibitory receptors (CD158 and CD158e), and activation and differentiation markers (CD62L and CD57) (Fig. S2). In contrast, NK cells did demonstrate increased expression of several markers following influenza virus exposure. Upregulated markers included activating receptors NKp30 and NKp44; an inhibitory receptor, NKG2A; activation markers CD25, CD26, Ki-67, CD69, and LAG-3; and transcription factors PLZF, Eomes, and T-bet (Fig. 4C and Fig. S2). The most dramatic change was in the expression of NK cell activation markers CD69, CD25, LAG-3, and CD26, which showed at least a 2-fold increase in both expression (as measured by the mean fluorescence intensity) and the frequency with which NK cells expressed the given marker (Fig. 4C). These results confirm that several activation markers were overexpressed in influenza virus-exposed NK cells (Fig. 4C), which corroborates the transcriptional data. Taken together, the RNA sequencing and phenotyping results suggest that these molecules may act as surrogate markers of increased NK cell functionality following influenza virus exposure.

Secreted factors in the supernatant are responsible for enhanced antibody-mediated NK cell functionality following exposure to influenza virus-infected cells. The RNA analyses suggested that cytokine/interferon signaling pathways are upregulated in NK cells cocultured with influenza virus-infected cells. This suggests that soluble factors likely drive the enhanced capacity of influenza virus-exposed NK cells to mediate antibody-dependent functions. As such, we performed Transwell experiments that coincubated PBMCs in the top portion of a Transwell with either infected or uninfected A549 cells in the bottom of the Transwell. Influenza virus-exposed and -unexposed NK cells were then tested for antibody-dependent activation. Despite physical separation from the influenza virus-infected cells, we still observed an increase in NK cell activation by both CD16 cross-linking and plate-bound HA-IgG immune complexes (Fig. 5A and B). To confirm this result, we performed supernatant transfer experiments with supernatants from infected or uninfected A549 cells. Following incubation with the transferred supernatants, PBMCs were washed, rested, and stimulated with plate-bound anti-CD16 antibody. Significantly higher frequencies of $CD107a^+$ and $CD107a^+$ IFN-γ^+ NK cells were observed following PBMC exposure to the supernatants of influenza virus-infected cells (Fig. 6A and B, respectively), supporting the results of the Transwell experiment.

To determine whether these results were specific to A549 cells, Transwell and supernatant transfer experiments were also performed with BEAS-2B cells. Consistent with the results of our Transwell experiment using A549 cells, PBMCs that were exposed to influenza virus-infected BEAS-2B cells had much greater frequencies of $CD107a^+$ and $CD107a^+$ IFN-γ^+ NK cells when stimulated with either anti-CD16 or plate-bound HA-IgG complexes (Fig. 5C and D). Supernatant transfer experiments with infected or uninfected BEAS-2B cells also corroborated the finding that soluble factors in the

FIG 4 Legend (Continued)
uninfected A549 cells from three separate PBMC donors. The top 100 differentially expressed genes of sorted NK cells exposed to infected or uninfected A549 cells are also listed in Table S1 in the supplemental material. (B) Significantly upregulated genes ($P < 0.05$, log FC > 2) in NK cells from influenza virus-exposed PBMCs were then clustered on the basis of their gene ontology to determine which pathways were the most upregulated. (C) Based on extensive flow cytometry phenotyping, four surface activation markers (CD69, CD25, CD26, and LAG-3) were found to be significantly upregulated on NK cells from influenza virus-exposed donor PBMCs ($n = 10$ donors). These activation markers were also shown to be upregulated by RNA sequencing in NK cells sorted from donor PBMCs ($n = 3$ donors). Groups were analyzed via Student *t* tests. **, $P < 0.05$. Bars represent mean values with SEM. MFI, mean fluorescence intensity.

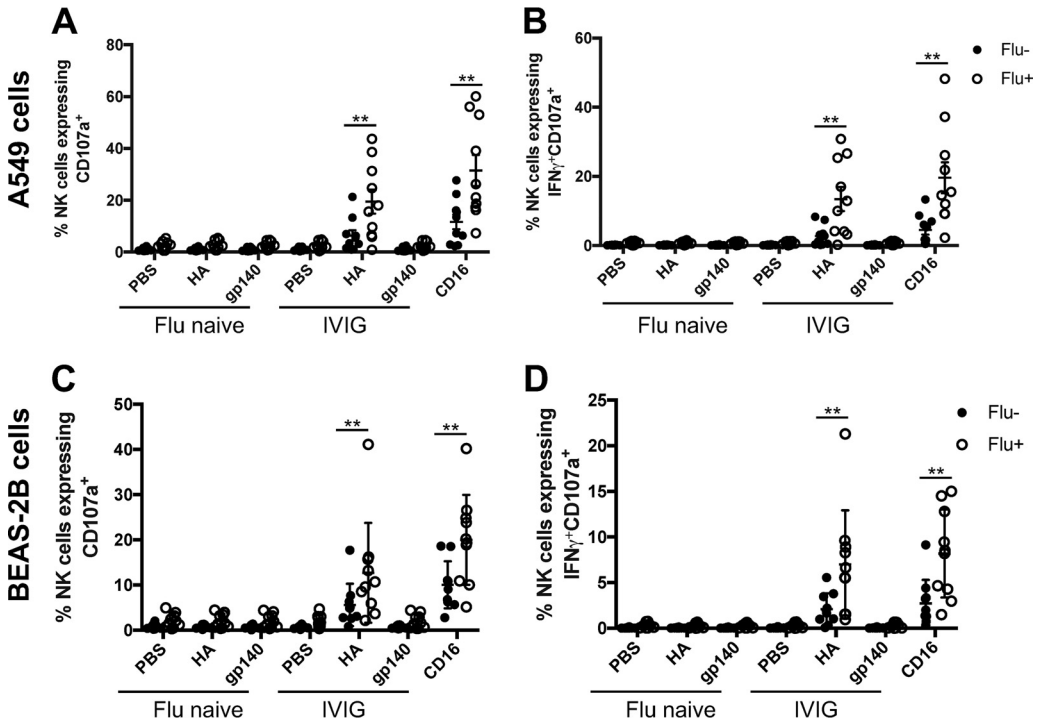

FIG 5 Increased antibody-mediated functionality of influenza virus-exposed NK cells is caused by factors released from infected cells. Healthy donor PBMCs ($n = 10$ donors) were added to the top section of a Transwell with infected or uninfected A549 cells (A, B) or BEAS-2B cells (C, D), which were incubated below in the lower section of the Transwell. PBMCs were then removed, washed, and rested for 12 h. NK cells in influenza virus-exposed (open circles) or -unexposed (solid circles) PBMCs were incubated with either plate-bound anti-CD16 antibody or plate-bound recombinant PR8 protein, HIV gp140, or PBS in the presence of IVIG (10 μg/ml) or naive macaque serum. NK cell activation was assessed via expression of CD107a alone (A, C) or CD107a and IFN-γ (B, D) by flow cytometry. Groups were analyzed by one-way ANOVA with Sidak's multiple-comparison test. **, $P < 0.05$. Bars represent mean values with SEM.

supernatant enhanced the capacity of NK cells to become activated in response to CD16 cross-linking and HA-IgG complexes (Fig. 6C and D). These results with BEAS-2B cells strengthened our argument that soluble factors in the supernatant are the likely cause of increased antibody-mediated NK cell functionality.

All the experiments described above were performed with whole PBMCs, and NK cells within the PBMC population were analyzed. To evaluate whether soluble factors released from influenza virus-infected cells directly modulated the capacity of NK cells to become activated or acted indirectly through other cell types within PBMCs, NK cells were purified (80% to 90% purity among the donors; data not shown) prior to incubation with supernatant from influenza virus-infected and -uninfected A549 cells. For purified NK cells, there was no significant difference in the frequency of $CD107a^+$ or $CD107a^+$ IFN-γ^+ NK cells between influenza virus-exposed and -unexposed NK cells following stimulation with plate-bound anti-CD16 (Fig. 6E and F). These data imply that factors released by influenza virus-infected cells act on other cell types within PBMCs to enhance the antibody-dependent functions of NK cells.

Free influenza virus in supernatant increases the antibody-dependent functionality of influenza virus-exposed NK cells. To establish whether influenza virus secreted into the supernatant from infected cells was the mediator of enhanced antibody-dependent NK cell functionality, we tested a range of influenza viruses added to PBMCs in the absence of influenza virus-infected cells. PBMCs were incubated either with H1N1 viruses (PR8 or A/California/07/2009 [H1N1] [CA/09]), H3N2 viruses (A/Switzerland/9715293/2013 [H3N2] [SW/13], A/Hong Kong/4801/2014 [H3N2] [HK/14]), or influenza virus type B (B/Brisbane/60/2008) or without virus. After washing and resting, the NK cells within the PBMCs were tested for functionality with plate-bound anti-CD16 antibody. All influenza viruses induced a significant increase in the frequency

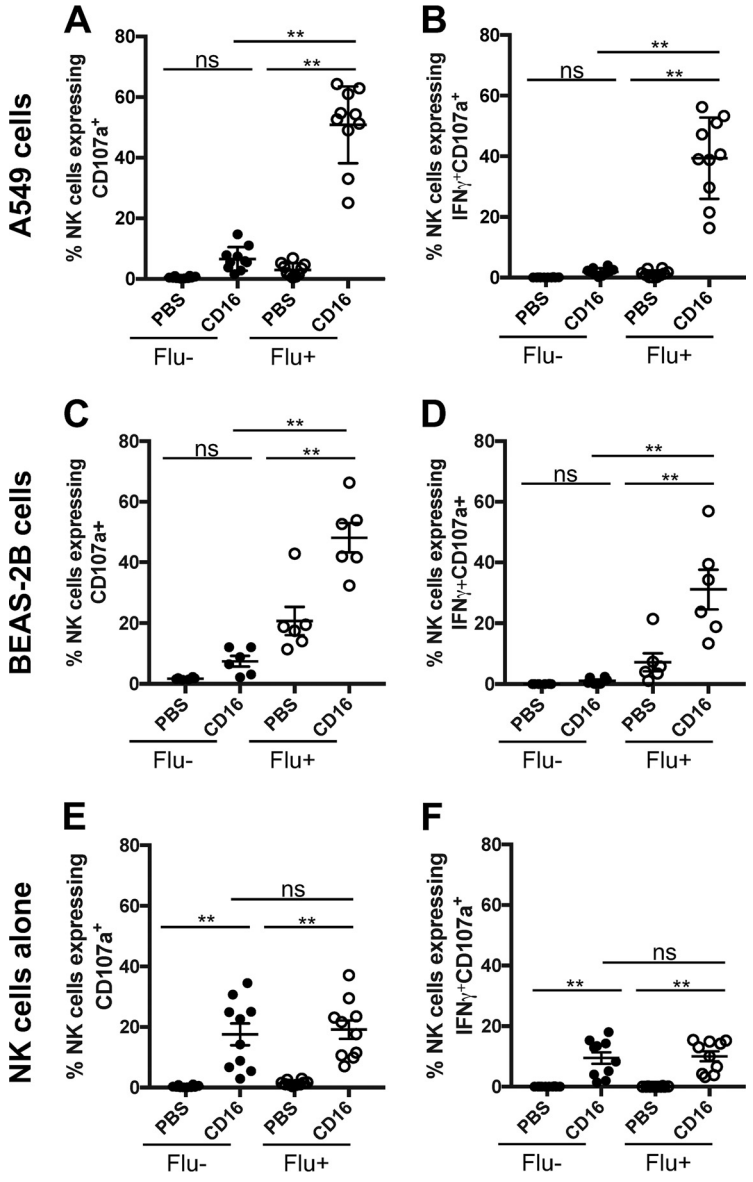

FIG 6 Supernatant transfer experiments from infected and uninfected A549 cells and BEAS-2B cells. Supernatants were collected from PR8-infected or uninfected A549 cells or BEAS-2B cells. The supernatants were then clarified by spinning at 1,000 × *g* for 10 min. Healthy donor PBMCs (A to D) or purified NK cells (E, F) were incubated with clarified supernatants from influenza virus-infected or uninfected A549 cells (A, B, E, F) or BEAS-2B cells (C, D). PBMCs were then removed, washed, and rested for 12 h. To measure the antibody-dependent activation potential, purified NK cells and NK cells in PBMCs were incubated with plate-bound anti-CD16 antibody (open circles) or uncoated wells (solid circles). NK cell activation was then assessed by expression of CD107a alone (A, C, E) or CD107a and IFN-γ (B, D, F) by flow cytometry. Groups were analyzed via one-way ANOVA with Sidak's multiple-comparison test. **, $P < 0.05$. Bars represent mean values with SEM.

of CD107a$^+$ and CD107a$^+$ IFN-γ$^+$ NK cells without significant differences between the five influenza viruses studied (Fig. 7A and B). To determine whether this effect was common to other RNA viruses, we incubated donor PBMCs with either PR8 influenza virus or respiratory syncytial virus (RSV). Both influenza virus- and RSV-exposed PBMCs enhanced NK cell functionality in response to CD16 cross-linking (Fig. 7C and D). The frequencies of activated NK cells were similar for both RSV and PR8 influenza virus, suggesting that a common pathway may be utilized by these RNA viruses to increase antibody-dependent NK cell functionality. Lastly, to determine the concentration of influenza virus required to achieve increased antibody-mediated NK cell functions,

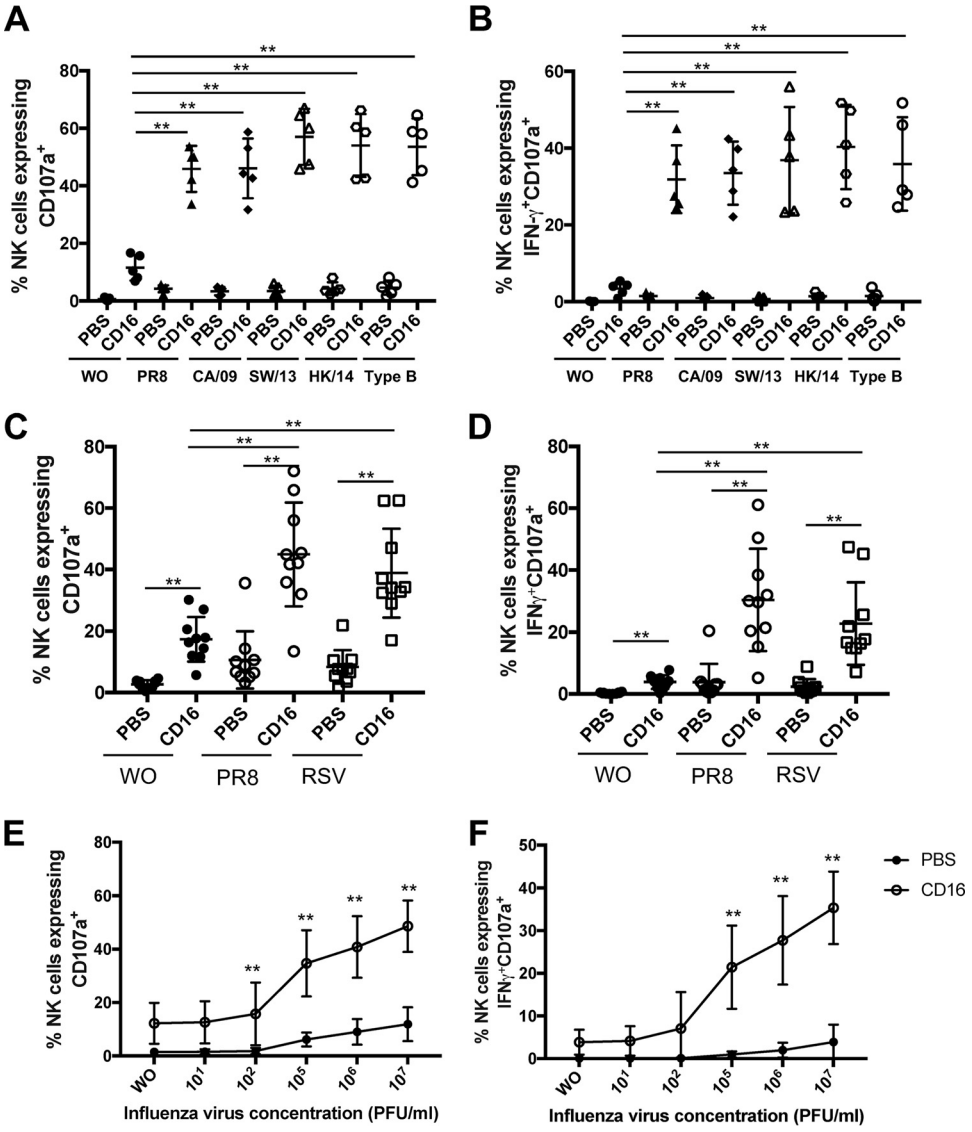

FIG 7 Increased antibody-mediated functionality of NK cells is mediated by virus released into supernatants. (A, B) Healthy donor PBMCs ($n = 5$ donors) were incubated with an egg-grown stock of 1×10^5 $TCID_{50}$/ml (without trypsin with dilution in R10 medium) of A/Puerto Rico/08/1934 (H1N1) (PR8), A/California/07/2009 (H1N1) (CA/09), A/Switzerland/9715293/2013 (H3N2) (SW/13), A/Hong Kong/4801/2014 (H3N2) (HK/14), or B/Brisbane/60/2008 (type B) or without (WO) influenza virus. (C, D) Healthy donor PBMCs ($n = 5$ donors) were incubated with or without an egg-grown stock of 10^4 PFU/ml of H1N1 PR8 or a cell-grown stock of 10^4 PFU/ml of RSV (strain A2) diluted in R10 medium. (E, F) Healthy donor PBMCs were incubated with or without different concentrations of an egg-grown stock of H1N1 PR8 ranging from 10^1 to 10^7 $TCID_{50}$/ml. In all cases, donor PBMCs were then removed, washed, and rested for 12 h. NK cell activation in virus-exposed (open symbols) or -unexposed (solid symbols) PBMCs was examined by incubation with plate-bound anti-CD16 antibody or uncoated wells. NK cell activation was then assessed by expression of CD107a alone (A, C, E) or CD107a and IFN-γ (B, D, F) using flow cytometry. Groups were analyzed via one-way ANOVA with Sidak's multiple-comparison test. **, $P < 0.05$. Bars represent mean values with SEM.

PBMCs were incubated with different concentrations of PR8 influenza virus. The increase in antibody-dependent NK cell responses occurred at concentrations of $>10^2$ 50% tissue culture infective dose ($TCID_{50}$)/ml, with functionality increasing as the titer of virus increased (Fig. 7E and F). Together, these results suggest that virus secreted into the supernatant by infected cells increased the antibody-dependent functions of NK cells within PBMCs.

The type I interferon pathway contributes to enhanced antibody-mediated NK cell responses after influenza virus exposure. The results described above suggest

that the secretion of intermediate cytokines by other cell types in PBMCs is responsible for increased antibody-mediated NK cell functions. We therefore assessed cytokine levels in supernatants from (i) influenza virus-infected and uninfected A549 cells alone, (ii) influenza virus-infected and uninfected A549 cells coincubated with PBMCs, and (iii) influenza virus-infected and uninfected A549 cells coincubated with PBMCs but with the supernatant removed after the PBMCs were rested alone following coincubation (Fig. 8A). We observed a significant increase in a number of pro-inflammatory cytokines, including IFN-γ-induced protein 10 (IP-10), macrophage inflammatory protein 1α/β (MIP-1α/β), RANTES, and SDF-1a, in the supernatants from influenza virus-infected A549 cells compared to those from uninfected A549 cells (Fig. 8A, left). Coincubation of PBMCs with influenza virus-infected A549 cells demonstrated an increase in the supernatant levels of IP-10, TNF, interleukin-1 (IL-1), IL-15, IL-31, IFN-α, IL-18, and IFN-γ relative to those demonstrated by coincubation of PBMCs with uninfected A549 cells (Fig. 8A, center). Furthermore, cytokines increased by coculture with influenza virus-infected A549 cells in postrest PBMC supernatants included those listed above, with the addition of IL-2 and granulocyte-macrophage colony-stimulating factor (GM-CSF) but the loss of IFN-α (Fig. 8A, right). To confirm the exposure of the cells to influenza virus, we also identified influenza virus-specific sequences in the influenza virus-exposed PBMCs shown in Fig. 8 (median, 1,302 mapped sequences/million reads) but not in the influenza virus-unexposed PBMCs (median, 1 mapped sequence/million reads).

To narrow down the list of candidate cytokines, we examined our RNA sequencing data from whole PBMCs (as opposed to NK cells only in Fig. 4B). The differential gene expression profile was generated for three donors using influenza virus-exposed and -unexposed whole PBMCs (Fig. 8B). The top 100 genes with a log fold change of greater than 2 or less than -2 and significant differential expression ($P < 0.05$) are listed in Table S2. Upregulated genes ($P < 0.05$, log FC > 2) were clustered based on pathways (Fig. 8C), and type I interferon pathways were clearly induced in influenza virus-exposed PBMCs. Given the upregulation of type I IFN-stimulated genes in influenza virus-exposed NK cells (Fig. 4B) and the increase in IFN-α after coincubation of PBMCs with influenza virus-infected A549 cells (Fig. 8A), type I IFN appeared to warrant further investigation.

To determine whether type I IFN was at least partially responsible for the observed increase in antibody-mediated NK cell functionality after influenza virus exposure, PBMCs were incubated with different concentrations of recombinant IFN-α and NK cells were subsequently tested for their activation potential via CD16 cross-linking. A significant increase in the frequency of activated NK cells was demonstrated following stimulation of PBMCs with recombinant IFN-α compared to that with no treatment (Fig. 9A and B; multiple *t* tests, $P < 0.001$). To confirm this finding, an interferon decoy receptor (B18R) was used to competitively block type I IFN binding in IFN-α-stimulated and influenza virus-exposed PBMCs. NK cell activation was significantly reduced in all samples containing the decoy IFN-α receptor (Fig. 9C and D), suggesting that type I interferon production by PBMCs contributes to the elevated antibody-dependent functionality of NK cells following influenza virus exposure.

To assess the role of upstream pattern recognition receptor (PRR) signaling, we incubated influenza virus-exposed PBMCs with the TLR/RIG-I inhibitor BX795 and measured NK cell activation by plate-bound anti-CD16 antibody. Interestingly, incubation with BX795 led to a modest reduction in the frequency of both CD107a$^+$ and CD107a$^+$ IFN-γ^+ NK cells in influenza virus-exposed PBMCs, but this did not reach statistical significance. No decrease in antibody-mediated NK cell activation was observed in influenza virus-unexposed PBMCs (Fig. 10A and B). Overall, these results suggest that antibody-mediated NK cell responses are increased by type I IFN production via the TLR/RIG-I signaling pathways.

Poly(I·C) stimulation increases NK cell functionality *in vitro* upon ligation of influenza virus-specific MAbs. TLR agonists are often used to increase antibody-mediated NK cell functionality in cancer immunotherapy. To study this in the context of influenza virus infection, PBMCs were incubated with poly(I·C), a TLR agonist that

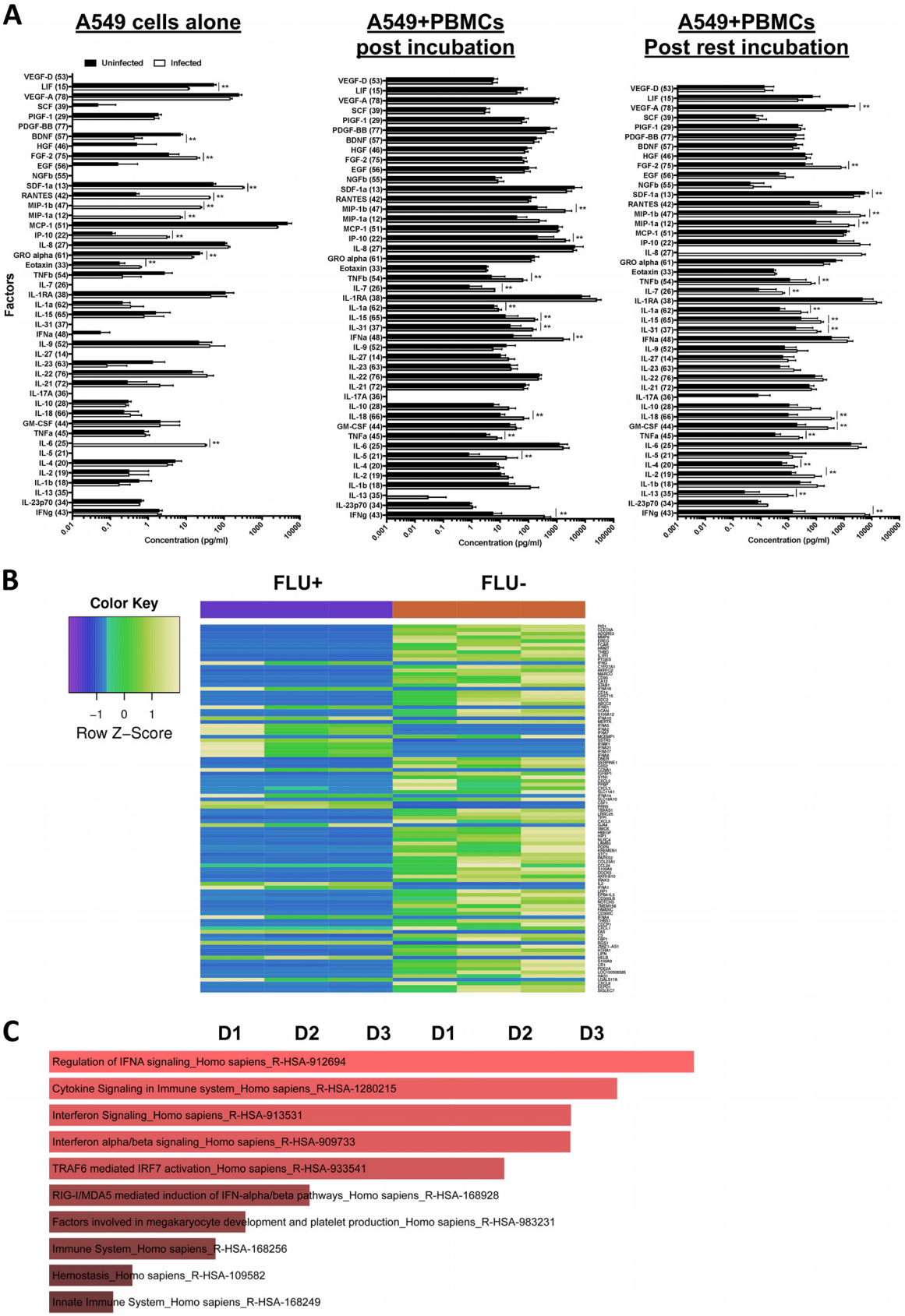

FIG 8 Supernatant cytokine multiplex and transcriptional analysis of PBMCs cocultured with influenza virus-infected cells. (A) Supernatants were collected from cells grown under the following conditions: (i) influenza virus-infected or uninfected A549 cells

(Continued on next page)

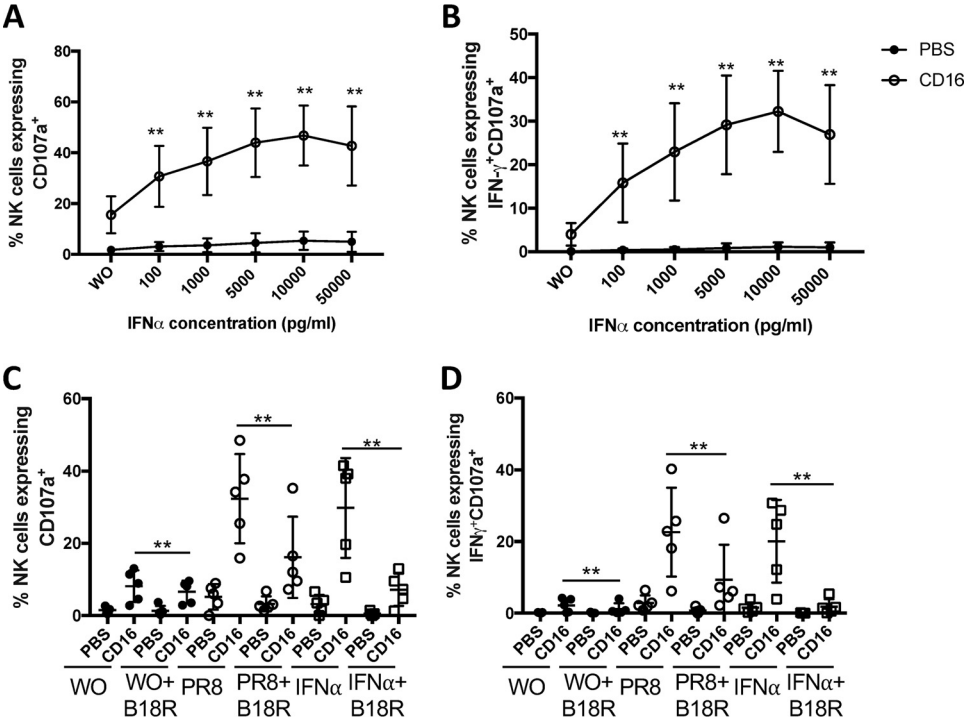

FIG 9 Type I interferon pathways are responsible for the enhanced antibody-dependent functionality of NK cells following influenza virus exposure. (A, B) Healthy donor PBMCs ($n = 10$ donors) were incubated with a range of concentrations (0, 100, 1,000, 5,000, 10,000, and 50,000 pg/ml) of recombinant IFN-α for 12 h. Healthy donor PBMCs were then removed, washed, and rested for 12 h. To assess the antibody-dependent activation potential, NK cells in PBMCs were then incubated with plate-bound anti-CD16 antibody (open circles) or uncoated wells (solid circles). NK cell activation was measured by expression of CD107a alone (A) or CD107a and IFN-γ (B) using flow cytometry. Groups were analyzed via one-way ANOVA, followed by Bonferroni's multiple-comparison test, with the IFN-α level compared to that without influenza virus. **, $P < 0.05$. Bars represent mean values with SEM. (C, D) Healthy donor PBMCs ($n = 5$ donors) were incubated without virus (solid circles), with 10^5 $TCID_{50}$/ml of PR8 virus (open circles), or with 50,000 pg/ml of IFN-α (open squares). For each condition, the incubations were performed with and without 1 μg/ml of type I IFN decoy receptor B18R. In all cases, the donor PBMCs were then removed, washed, and rested for 12 h. To measure the activation potential, NK cells in PBMCs were incubated with either plate-bound anti-CD16 antibody or uncoated wells. NK cell activation was measured by expression of CD107a alone (C) or CD107a and IFN-γ (D) by flow cytometry. Groups were analyzed via one-way ANOVA, followed by Sidak's multiple-comparison test. **, $P < 0.05$. Bars represent mean values with SEM.

stimulates type I IFN secretion through the TLR3 pathway. We observed a dose-dependent increase in the frequency of activated NK cells by CD16 cross-linking as the concentration of poly(I·C) increased from 3.125 μg/ml to 50 μg/ml (Fig. 11A and B). These results suggest that influenza virus could be acting through TLR signaling to induce type I IFN production, which in turn increases antibody-mediated NK cell functionality.

FIG 8 Legend (Continued)

incubated alone for 12 h (left), (ii) influenza virus-infected or uninfected A549 cells coincubated with healthy donor PBMCs ($n = 10$ donors) for 12 h (middle), and (iii) influenza virus-infected or uninfected A549 cells coincubated with healthy donor PBMCs for 12 h but with the supernatant removed after PBMCs were rested alone for 12 h following coincubation (right). The cytokines/chemokines in the supernatants were measured using a Luminex 45-plex array, and the concentrations of each cytokine/chemokine were determined by reference to the kit standards. Live sorted PBMCs ($n = 3$ donors) exposed to infected or uninfected A549 cells were tested for differential gene expression by RNAseq. VEGF, vascular endothelial growth factor; LIF, leukemia inhibitory factor; PlGF, placental growth factor; PDGF, platelet-derived growth factor; BDNF, brain-derived neurotrophic factor; HGF, hepatocyte growth factor; FGF-2, fibroblast growth factor 2; EGF, epidermal growth factor; NGFb, nerve growth factor β; MCP-1, monocyte chemotactic protein 1; IL-1RA, IL-1 receptor antagonist. (B) Transcriptional profile based on the top 100 differentially expressed genes of whole PBMCs from three separate donors previously exposed to infected or uninfected A549 cells. The top 100 differentially expressed genes of whole PBMCs exposed to infected or uninfected A549s are also listed in Table S2 in the supplemental material. (C) Significantly upregulated genes ($P < 0.05$, log FC > 2) in influenza virus-exposed PBMCs were then clustered on the basis of their gene ontology to determine which pathways were the most upregulated. Groups were analyzed via one-way ANOVA with Sidak's multiple-comparison test. **, $P < 0.05$. Bars represent mean values with SEM.

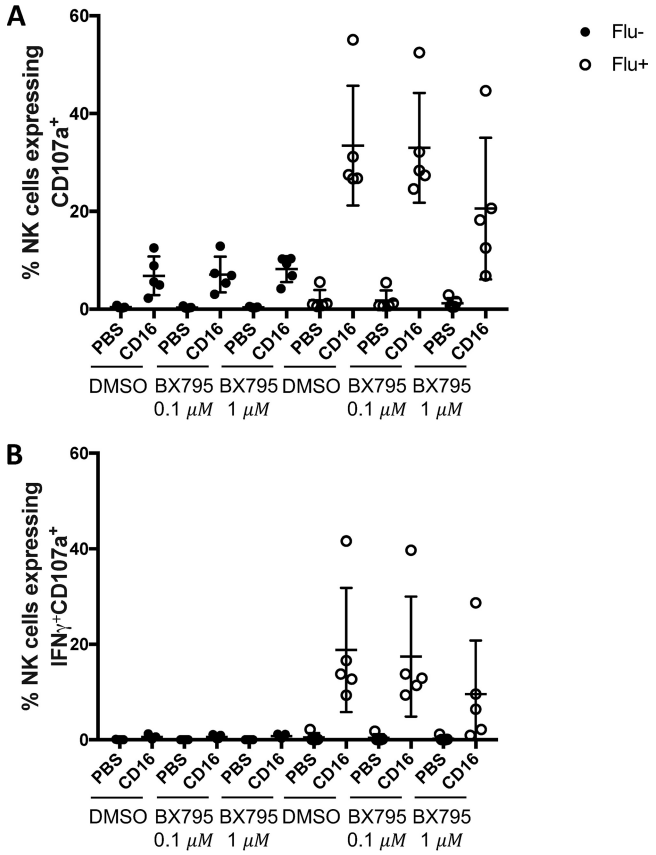

FIG 10 Inhibition of TLR signaling decreases antibody-dependent NK cell functionality. Healthy donor PBMCs ($n = 5$ donors) were incubated with (open circles) or without (solid circles) 1×10^5 PFU of A/Puerto Rico/08/1934 (H1N1) (PR8) virus for 12 h in the presence of either DMSO (negative control) or 0.1 μM or 1 μM of BX795 inhibitor. Subsequently, donor PBMCs were washed and rested for 12 h, once again in the presence of DMSO or inhibitor. To measure antibody-mediated activation, NK cells in PBMCs were incubated with plate-bound anti-CD16 antibody and NK cell activation was measured by expression of CD107a alone (A) or CD107a and IFN-γ (B) using flow cytometry.

Given that poly(I·C) increased antibody-dependent NK cell activation following stimulation with anti-CD16 antibody, we postulated that the addition of poly(I·C) to PBMCs would also enhance NK cell activation by plate-bound HA-IgG complexes with either polyclonal anti-influenza virus antibodies from IVIG or a monoclonal antibody targeting the HA stem region (Fig. 11C and D). A significant increase in the frequency of CD107a$^+$ and CD107a$^+$ IFN-γ^+ NK cells was observed in poly(I·C)-stimulated PBMCs incubated with plate-bound immune complexes containing CR9114 or IVIG. Indeed, the frequency of activated NK cells was marginally higher for poly(I·C)-stimulated PBMCs incubated with CR9114 than for those incubated with IVIG, a difference that was negligible in PBMCs that were not stimulated with poly(I·C). These results show that direct TLR stimulation by TLR agonists can enhance NK cell activation by influenza virus-specific antibodies.

DISCUSSION

In this study, we showed that influenza virus virions released from infected cells led to type I IFN production, which increased the capacity of NK cells to mediate antibody-dependent responses. Manipulating the type I IFN pathway through the addition of TLR agonists and TLR inhibitors altered the magnitude of antibody-dependent NK cell activation, illustrating the potential to enhance or dampen the potency of influenza virus-specific antibody immunotherapies.

Type I IFN is critical for limiting virus replication early after infection. Influenza virus stimulates the production of type I IFN through TLR7 (29), TLR3 (30, 31), and RIG-I (32).

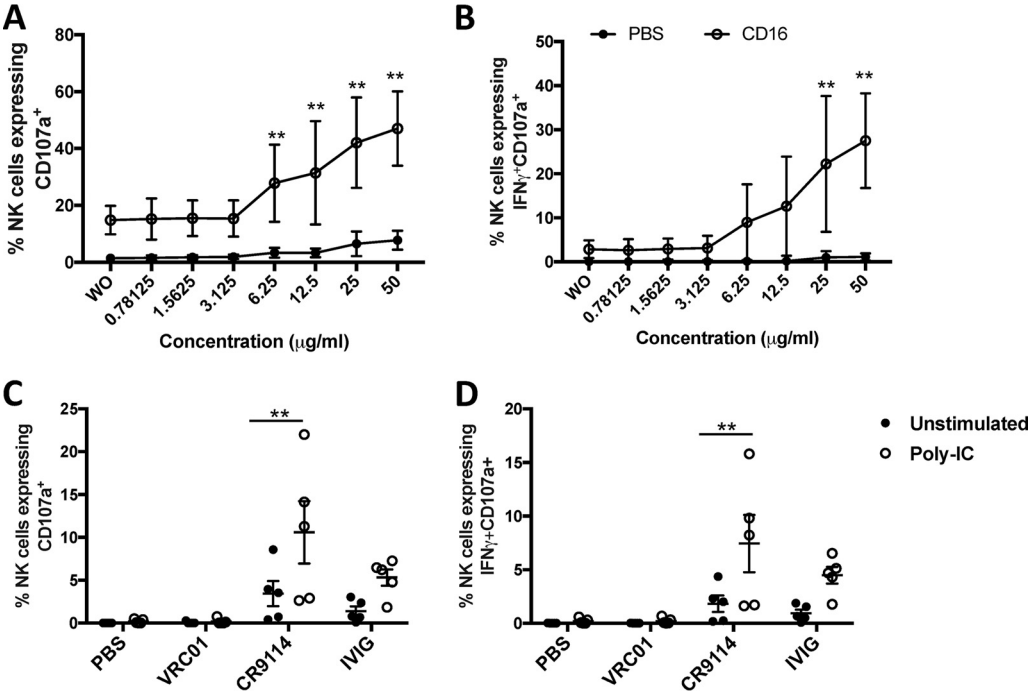

FIG 11 Stem-specific ADCC responses were increased following poly(I·C) stimulation of PBMCs. (A, B) Healthy donor PBMCs ($n = 10$ donors) were incubated with or without 2-fold dilutions of poly(I·C) from 0.78125 to 50 μg/ml for 12 h. Following incubation, donor PBMCs were washed and rested for 12 h. To measure the antibody-dependent activation potential, NK cells in donor PBMCs were incubated with either plate-bound anti-CD16 antibody (open circles) or uncoated wells (solid circles). NK cell activation was then assessed by expression of CD107a alone (A) or CD107a and IFN-γ (B) by flow cytometry. Groups were analyzed via one-way ANOVA, followed by Bonferroni's multiple-comparison test, with the IFN-α level compared to that without influenza virus. **, $P < 0.05$. Bars represent mean values with SEM. (C, D) Healthy donor PBMCs ($n = 10$ donors) were incubated with (solid circles) or without (open circles) poly(I·C) at 50 μg/ml for 12 h. Donor PBMCs were then washed and rested for 12 h. To measure the antibody-mediated activation potential, NK cells in PBMCs were incubated with recombinant HA (A/Puerto Rico/08/1934)-coated plates in the presence of either PBS, VRC01 (100 μg/ml), CR9114 (100 μg/ml), or IVIG (100 μg/ml). NK cell activation was measured via expression of CD107a (C) or CD107a and IFN-γ (D) by flow cytometry. Groups were analyzed via two-way ANOVA followed by Sidak's multiple-comparison test. **, $P < 0.05$. Bars represent mean values with SEM.

Plasmacytoid dendritic cells (pDCs) are primarily responsible for type I IFN production via the TLR7 pathway, while RIG-I and TLR3 drive type I IFN production by non-pDC types (33, 34). Human NK cells express a variety of TLRs, including TLR3, TLR7, and TLR8, but NK cells commonly require cytokines produced by accessory cells to become activated by TLR agonists and pathogen-associated molecular patterns (35, 36). This is consistent with our finding that free virus released into the supernatant by influenza virus-infected cells did not increase the antibody-dependent activation of purified NK cells. Indeed, we showed that free virus stimulated type I IFN production by other cells in the PBMCs, leading to indirect activation of antibody-mediated NK cell responses. Downstream activation of NK cells by type I IFN released from other cell types was also supported by our transcriptional data, which showed that type I IFN-inducible genes and transcription factors were preferentially upregulated in influenza virus-exposed PBMCs and NK cells. This study focused primarily on the stimulation of antibody-dependent NK cell functions by type I IFN, but this does not exclude the possibility of the involvement of other cytokines. Our cytokine array and RNA sequencing data showed that IL-18 was upregulated in influenza virus-exposed PBMCs, suggesting that it may also contribute to enhanced antibody-dependent NK cell activation.

Influenza virus has a number of type I IFN evasion mechanisms, including antagonism of RIG-I by the NS1 protein. Infecting strains of influenza virus have differential capacities to block IFN-β transcription via the RIG-I pathway, with the PR8 and H1N1pdm09 influenza viruses being the most efficient (25). This likely explains the lack of type I IFN production by PR8-infected respiratory epithelial cells in our study, as

shown in the cytokine multiplex. Another immune evasion strategy involves influenza virus directly infecting and killing NK cells. However, in this study, we observed low to undetectable levels of influenza virus-infected NK cells. The low levels of NK cell infection were likely the result of PBMC incubations in complete medium containing high concentrations of fetal calf serum and lacking trypsin. The fact that this immune evasion strategy employed by influenza virus may have been hindered in our culture system is a limitation of our study. Follow-up studies investigating antibody-dependent NK cell activation during influenza virus infection could be performed in animal models under *in vivo* conditions, where all relevant enzymes would be present.

A variety of MAbs targeting highly conserved regions of HA have been isolated in recent years (14, 37, 38). Many of these MAbs have been shown to require Fc-mediated effector functions, in particular, ADCC, to protect mice from lethal influenza virus challenge (9, 10, 14). The prophylactic and therapeutic potentials of HA stem-specific MAbs are currently being assessed in human trials. An understanding of the major factors that can influence ADCC by HA stem-specific MAbs is important to assess their utility and potential drawbacks for the treatment or prevention of influenza virus infection. The potency of ADCC mediated by passively transferred antibodies is determined, at least in part, by the functionality of host NK cells. Herein, we showed that type I IFN plays a key role in enhancing antibody-dependent NK cell functionality during influenza virus infection. Since type I interferon pathways can be readily manipulated by the addition of TLR agonists or inhibitors, the ADCC activity of IVIG or influenza virus-specific MAbs could be enhanced or dampened for therapeutic use. Furthermore, we identified surrogate markers of increased NK cell functionality, including CD69, CD25, Ki-67, LAG-3, and CD26, on influenza virus-exposed NK cells by transcriptional and phenotypic analyses. Increased expression of these activation markers may suggest a primed state of NK cells brought about by type I IFN secretion from accessory cells. Screening for these markers prior to the administration of MAb immunotherapy to influenza virus-infected patients could provide valuable insight into which subjects are capable of mounting a robust ADCC response. In mouse models of influenza, macrophages are known to be important for Fc receptor-dependent protection by influenza virus-specific bNAbs (15). Influenza virus-specific ADP is also induced by both influenza vaccination and infection in humans, but its role in protective immunity remains unclear (39, 40). Future studies investigating the role of primary macrophages and ADP are necessary to understand the contribution of other cell types and Fc-mediated effector functions during human influenza virus infection.

Prior studies by our group and others have shown that cross-reactive ADCC-mediating antibodies are present in humans and are expanded following influenza vaccination and influenza virus infection (41). Herein, we show that NK cells gain antibody-dependent functionality via type I IFN release during the course of influenza virus infection, which may enhance the ADCC response *in vivo*. These findings suggest that the limiting factor for influenza virus-specific ADCC may not be NK cell functionality. Instead, other factors, such as the concentration of ADCC-mediating antibodies in the respiratory tract or inhibition of ADCC by hemagglutination inhibition antibodies, may be important in determining the potency of an ADCC response during influenza virus infection (42, 43). Influenza virus infection results in the priming of NK cells, which may lead to the more efficient clearance of infected cells by ADCC. As such, *in vitro* studies performed with heterologous NK cells lacking this primed phenotype may not accurately reflect the true protective potential of ADCC antibodies during influenza virus infection *in vivo*.

NK cells can be protective or immunopathological in mice, depending on the infectious dose of influenza virus. NK cells are important for the survival of mice following primary influenza virus infection (44, 45), but mice inoculated with higher doses of influenza virus have enhanced NK cell-mediated immunopathology. NK cell-depleted mice given higher doses of influenza virus demonstrated better survival rates than wild-type mice inoculated with 10-fold less influenza virus (46, 47). Based on our results, we speculate that higher doses of influenza virus may confer NK cells with

greater functionality via increased type I IFN release. The potential for NK cell-mediated immunopathology presents a major concern, particularly for the therapeutic use of HA MAbs with ADCC activity. The delicate balance between enhancing protection and causing immunopathology remains poorly characterized in the context of influenza virus-specific ADCC. Our work needs to be complemented with *in vivo* studies to show that the passive transfer of HA MAbs will confer a greater protective capacity during influenza virus challenge and not result in immunopathology.

In conclusion, we found that influenza virus-infected cells release free virus into the supernatant, initiating type I IFN production from PBMCs, which primes NK cells for antibody-mediated activation. These primed NK cells demonstrate higher levels of antibody-mediated degranulation and cytokine production than influenza virus-unexposed NK cells. This priming can be recapitulated by the addition of TLR agonists that stimulate type I IFN production and indirectly increase NK cell functionality following antibody engagement (by either therapeutic MAbs or naturally occurring antibodies). Overall, this study highlights an important mechanism by which the antibody-mediated functions of NK cells can be primed to respond to influenza virus infection.

MATERIALS AND METHODS

PBMCs from healthy human subjects. Buffy coat preparations from healthy blood donors were kindly provided by the Red Cross Blood Service (Melbourne, Victoria, Australia). PBMCs were isolated by use of a Ficoll gradient (GE Healthcare, ISU, Chicago, IL) and stored in liquid nitrogen. Frozen PBMCs were rapidly thawed at 37°C, washed twice in RPMI medium, and suspended at a concentration of 10^7 cells/ml in R10 medium (RPMI 1640 medium containing 10% fetal bovine serum, 2 mmol/liter L-glutamine, 50 IU/ml penicillin, 50 μg/ml streptomycin; all from Gibco, Life Technologies) for use in coculture assays.

Virus and recombinant influenza virus proteins. Egg-grown stocks of influenza A/Puerto Rico/08/1934 (H1N1), A/California/07/2009 (H1N1pdm09), A/Switzerland/9715293/2013 (H3N2), A/Hong Kong/4801/2014 (H3N2), or B/Brisbane/60/2008 virus were used to infect either a human alveolar cell line (A549) or a human bronchus epithelial cell line (BEAS-2B) (A549 and BEAS-2B cells were kindly provided by Sarah Londrigan and Patrick Reading). Virus was titrated by the standard $TCID_{50}$ method, as previously described (48). Respiratory syncytial virus (RSV) A2 virus was kindly provided by Patrick Reading and Fernando Villalon (University of Melbourne). HA protein (A/Puerto Rico/08/1934 H1N1) was purchased from Sinobiological (China), and anti-human LEAF-purified CD16 (clone 3G8) was purchased from BioLegend (San Diego CA).

Conditions for coculture of PBMCs with infected cells. Adherent A549 or BEAS-2B cells (80% confluent) were cultured with or without 10^5 $TCID_{50}$ of influenza virus in 1 ml of Opti-minimum essential medium (Opti-MEM; Gibco, Life Technologies) and incubated at 37°C with 5% CO_2. After 1 h, adherent cells were washed twice with phosphate-buffered saline (PBS) and incubated with 10^7 PBMCs per well in R10 medium for 12 h at 37°C with 5% CO_2. Following the 12-h incubation, infection of A549 or BEAS-2B cells was confirmed by assessing the presence of cytopathic effects (CPE) and by trypsinizing (using trypsin-Versene; Department of Microbiology and Immunology, Media Preparation Unit) and staining with either anti-NP fluorescein isothiocyanate (FITC; clone 431; Abcam) or anti-M2 allophycocyanin (APC) antibodies (an in-house direct conjugate of Abcam clone 14C2). Cells were confirmed to have more than 80% infection by flow cytometry (data not shown). PBMCs were removed from the plates, washed 3 to 4 times with RPMI medium, and plated or rested for at least 12 h at 37°C with 5% CO_2 (or as indicated in the figure legends). NK cells within the PBMCs were then tested for functionality. The purpose of this resting period was to examine the functionality of influenza virus-exposed NK cells independently of direct exposure to the virus and assess the duration of this effect in the absence of ongoing infection, both of which are important factors for translating this work into animal models and humans.

To test whether direct contact between influenza virus-infected A549 cells and PBMCs was required for enhanced antibody-dependent NK cell functionality, 12-well Transwell plates containing polyester membrane cell culture inserts (Corning) were used. PBMCs (10^7) were plated on the top portion of the Transwell, and infected or uninfected A549 or BEAS-2B cells were plated on the bottom of the Transwell, which was then incubated for 12 h at 37°C with 5% CO_2. PBMCs were then removed from the top of the Transwell and treated as described above.

In another variation of the assay, A549 or BEAS-2B cells were infected with influenza virus as described above, but following the 1-h incubation, the cells were washed twice with PBS and incubated in R10 medium for 12 h at 37°C with 5% CO_2. Next, supernatants from both infected and uninfected cells were removed and centrifuged at 1,000 $\times$ *g* for 10 min to remove dead or dislocated cells. Supernatants were then added to 10^7 thawed PBMCs, and the mixture was incubated for 12 h at 37°C with 5% CO_2. Following incubation with the supernatants, the PBMCs were removed and treated as described above.

Conditions for stimulation of PBMCs with viruses and cytokines. In experiments performed with multiple concentrations of influenza virus, PBMCs were incubated with or without different concentrations of A/Puerto Rico/08/1934 (H1N1) (PR8) virus ranging from 10^1 to 10^7 50% tissue culture infective doses ($TCID_{50}$)/ml in R10 medium. For assays comparing different strains of influenza virus, PBMCs were washed in R10 medium and incubated with or without 10^5 $TCID_{50}$/ml of various influenza viruses

(without trypsin and with dilution in R10 medium), including A/Puerto Rico/08/1934 (H1N1) (PR8), A/California/07/2009 (H1N1) (CA/09), A/Switzerland/9715293/2013 (H3N2) (SW/13), A/Hong Kong/4801/2014 (H3N2) (HK/14), and B/Brisbane/80/2008 (influenza virus type B). In experiments comparing influenza virus and RSV, PBMCs were incubated with or without 10^4 PFU/ml of egg-grown PR8 influenza virus or 10^4 PFU/ml of cell-grown RSV (strain A2) diluted in R10 medium. For Toll-like receptor (TLR) inhibitor experiments, PBMCs were incubated with or without 10^5 PFU of PR8 virus for 12 h in the presence of either dimethyl sulfoxide (DMSO; negative control) or 0.1 μM or 1 μM BX795 inhibitor (catalog number tlrl-bx7; InvivoGen). To test for cytokine stimulation, PBMCs were incubated with 100 to 50,000 pg/ml of human recombinant IFN-α 2a (Sigma). For experiments performed with the type I IFN decoy receptor B18R, PBMCs were left unstimulated or were stimulated with 10^5 $TCID_{50}$/ml of PR8 or 50,000 pg/ml of IFN-α in the presence or absence of 1 μg/ml of type I interferon decoy receptor B18R (StemCell Technologies). Poly(I·C) stimulation was tested by incubating PBMCs with or without 2-fold dilutions of poly(I·C) ranging from 0.78125 to 50 μg/ml (InvivoGen, Life Technologies). In assays performed with a single dilution of poly (I·C), PBMCs were incubated with or without 50 μg/ml of poly(I·C). Thawed donor PBMCs were used in all assays, and the PBMCs were incubated for 12 h at 37°C with 5% CO_2 under each of the experimental conditions described above. Following the 12-h incubation, PBMCs were washed and rested for 12 h before functional characterization. After resting, the NK cells in the PBMCs were tested for functionality using the plate-bound NK cell activation assay (described below).

Plate-bound NK cell activation assay. NK cell activation was measured as previously described (41, 49). Briefly, 96-well enzyme-linked immunosorbent assay (ELISA) plates were coated with 400 ng/well of recombinant HA protein or anti-human CD16 overnight at 4°C. Following washing, pooled human intravenous immunoglobulin (IVIG; 100 μg/ml; Intragam-P; CSL Behring) was used as a source of polyclonal anti-influenza virus antibodies, and serum from an influenza virus-naive pigtail macaque (1:100) was used as a negative control. In some instances, the MAb VRC01 and HA stem-specific bNAb CR9114 were used at a concentration of 100 μg/ml (both were kindly provided by Adam Wheatley, University of Melbourne). Antibody was added to the plates for 2 h at 37°C. The plates were then washed, and 10^6 PBMCs were added in the presence of 5 μg/ml brefeldin A (Sigma-Aldrich) and 5 μg/ml monensin (Golgi Stop; BD) for 5 h at 37°C with 5% CO_2. After incubation, the cells were stained with Aqua LIVE/DEAD (Thermo Fisher), anti-CD56 phycoerythrin (PE)-Cy7 (clone NAM16.2; BD), anti-CD3 peridinin chlorophyll protein (PerCP; clone SK7; BD), and anti-CD107a APC-Cy7 (clone H4A3; BioLegend) for 30 min at 4°C and fixed with 1% paraformaldehyde (Sigma-Aldrich) for 10 min at room temperature. The cells were then permeabilized by a 10-min incubation in Perm-2 solution (BD) at room temperature. The cells were washed with PBS and incubated with anti-IFN-γ APC (clone B27; BD) and anti-TNF BV421 (clone Mab11; BD). In some cases, anti-NP fluorescein isothiocyanate (FITC; clone 431; Abcam) was also used to test for infection of PBMCs. The frequency of $CD3^-$ $CD56^+$ NK cells was assessed for $CD107a^+$ alone as an indicator of total functional activation of cells and double ($CD107a^+$ IFN-γ^+)-positive NK cells as an indicator of polyfunctionality. Cells were analyzed on either a FACSCanto II or LSRFortessa flow cytometer (BD). Analysis was performed on FlowJo software (version 9.9.5).

Target cell-based NK cell activation assay. Direct activation of NK cells was assessed by incubation of PBMCs with the MHC class I-deficient lymphoblastic cell line 721.221 or K562 (ATCC CRL-1855 and CCL-243, respectively; both were provided by Andrew Brooks, University of Melbourne). Antibody-dependent NK cell activation was assessed by incubation of PBMCs with 721.221 cells in the presence of rituximab (final concentration, 10 μg/ml; Roche, NSW, Australia). PBMCs were used as effectors cells. Briefly, PBMCs (from 10 donors) were coincubated for 12 h with infected or uninfected A549 cells. Next, PBMCs were isolated, washed three times with RPMI medium, and rested for 12 h at 37°C with 5% CO_2. Following resting, PBMCs were washed with RPMI medium, counted with an automated cell counter (Abbott Cell-Dyn Emerald), resuspended into R10 medium, and incubated alone (10^6 cells) with K562 or 721.221 cells at effector-to-target cell ratios of 1:1, 10:1, or 100:1 in the presence of 5 μg/ml brefeldin A (Sigma-Aldrich) and 5 μg/ml monensin (Golgi Stop; BD) for 5 h. For antibody-dependent assays, rituximab was also added to the coculture of PBMCs and target cells prior to incubation. After incubation, the cells were stained with Aqua LIVE/DEAD (Thermo Fisher), anti-CD56 PE-Cy7 (clone NAM16.2; BD), anti-CD3 PerCP (clone SK7; BD), and anti-CD107a APC-Cy7 (clone H4A3; BioLegend) for 30 min at 4°C and fixed with 1% paraformaldehyde (Sigma-Aldrich) for 10 min at room temperature. The cells were then permeabilized by a 10-min incubation in Perm-2 solution (BD) at room temperature, washed with PBS, and incubated with anti-IFN-γ APC (clone B27; BD). NK cells in PBMCs were studied for activation by flow cytometry as described above.

Target cell killing assay. To evaluate the functional capacity of influenza virus-exposed NK cells, a lactate dehydrogenase (LDH) assay was employed to assess target cell killing. PBMCs from three donors were cultured with or without 10^5 $TCID_{50}$/ml of PR8 for 12 h. Following a 12-h rest period, NK cells were negatively selected using an EasySep human NK cell isolation kit (StemCell Technologies) according to the manufacturer's instructions. Isolated NK cells (effectors, 2.0×10^4) were then added to 96-well round-bottom tissue culture plates with 721.221 target cells (2.0×10^4) in a 1:1 effector-to-target cell ratio. LDH release was quantitated using a CytoTox 96 nonradioactive cytotoxicity assay (Promega) according to the manufacturer's instructions. Briefly, the plates were centrifuged at $250 \times g$ for 4 min, and lysis solution was added to control wells with 721.211 cells only before incubation at 37°C for 4 h. Following an additional centrifugation at $250 \times g$ for 4 min, 50 μl/well supernatant was transferred to a 96-well flat-bottom Nunc MaxiSorp ELISA plate (Thermo Fisher) and 50 μl/well of substrate was added. After 30 min, 50 μl of stop solution was added to every well and the absorbance was measured at 492 nm. Percent cytotoxicity was calculated using absorbance readings from which the background for R10 medium only was subtracted with the following formula: [(experimental LDH release – effector cell

spontaneous LDH release – target spontaneous LDH release)/(target maximum LDH release – target spontaneous LDH release)] × 100. Maximum LDH release was determined from control 721.221 cells with lysis solution, and spontaneous LDH release for each cell type and number was determined by incubation of 721.221 and NK cells alone.

Luminex 45-plex cytokine analysis. Supernatants from cells under the following three conditions were collected and stored at −80°C for multiplex cytokine analysis: (i) A549 cells either uninfected or infected with influenza virus for 12 h (repeat of four individual experiments), (ii) uninfected or influenza virus-infected A549 cells coincubated with donor PBMCs (from 10 randomized donors) for 12 h, and (iii) uninfected or influenza virus-infected A549 cells coincubated with donor PBMCs (from the same 10 randomized donors) for 12 h, followed by washing and incubation (or resting) of PBMCs alone for 12 h. The Luminex cytokine/chemokine/growth factor 45-plex human ProcartaPlex Panel 1 (Thermo Fisher Scientific) assay was performed per user specifications using stored supernatants. Briefly, the plates were washed using a Bio-Plex Pro II wash station and read on a Bio-Plex200 reader (Bio-Rad). Binding of the PE detector antibodies was measured at the specific bead regions, and the mean fluorescence intensity was determined for each cytokine. Standards were run for all cytokines used, and the concentration was extrapolated from the data using Bio-Plex Manager software (Bio-Rad).

Multiparameter phenotyping. Cell surface and intracellular phenotyping was performed on donor PBMC samples that were incubated with infected or uninfected A549 cells for 12 h, washed, and rested for 24 h at 37°C with 5% CO_2. Cells were stained with the following human surface markers: LIVE/DEAD fixable Blue (Thermo Fisher Scientific), anti-CD16 FITC (clone 3G8; BD), anti-CD158 APC (KIR2DL1/S1/S3/S5; clone HP-MA4; BioLegend), anti-CD159c (NKG2C) Alexa Fluor 700 (clone 134591; R&D Systems), anti-CD57 APC-Vio770 (clone TB03; Miltenyi Biotec), anti-CD336 (NKp44) BUV395 (clone p44-8; BD), anti-CD56 BUV737 (clone NCAM16.2; BD), anti-CD3 BUV805 (clone SK7; BD), anti-CD223 (LAG-3) BV421 (clone LAG-3; BD), anti-CD158e1 (KIR3DL1) BV605 (clone DX9; BD), anti-CD337 (NKp30) BV711 (clone p30-15; BD), anti-CD335 (NKp46) BV786 (clone 9E2; BD), anti-CD159a (NKG2A) PE (clone Z199; Beckman Coulter), anti-CD314 (NKG2D) PE-Cy7 (clone 1D11; BioLegend), anti-CD26 APC (clone BA5b; BioLegend), anti-CD25 APC-R700 (clone 2A3; BD), anti-CD69 (clone FN50; BD), and anti-CD62L BV785 (clone DREG-56; BioLegend). Following permeabilization using a transcriptional factor buffer set (BD), staining was performed with the following intracellular antibodies: anti-Eomes PerCP-eFluor 710 (clone WD1928; Life Technologies), anti-Ki-67 Alexa Fluor 647 (clone Ki-67; BioLegend), anti-T-bet BV421 (clone 4B10; BioLegend), anti-granzyme B BV510 (clone GB11; BD), and anti-PLZF PE-CF594 (clone R17-809; BD). Cells were analyzed using an LSRFortessa flow cytometer (BD). Analysis was performed on FlowJo software (version 9.9.5).

RNA sequencing and analysis. PBMCs from three donors were stained with the following human surface markers: Aqua LIVE/DEAD (Thermo Fisher), anti-CD56 PE-Cy7 (clone NAM16.2; BD), and anti-CD3 PerCP (clone SK7; BD). Stained cells were resuspended in Opti-MEM (Gibco, Life Technologies) prior to cell sorting. LIVE/DEAD-negative target cell populations were gated on. Live $CD3^-$ $CD56^+$ NK cells (10^5) were immediately sorted into RLT buffer (Qiagen) containing 0.14 M β-mercaptoethanol (Sigma) using a FACSAria III cell sorter. Sorted cells were maintained at a 3.5 volume ratio of RLT buffer to sorted solution postsorting. Genomic DNA was removed using a genomic DNA eliminator (Qiagen) per the manufacturer's protocol. Two hundred fifty microliters of 100% ethanol was added to every 350-μl volume of flowthrough solution, and the resulting RNA solution was processed per the RNeasy Plus microkit protocol (Qiagen). RNA sequencing (RNAseq) was done with an Illumina HiSeq 2500 instrument at the Australian Genome Research Facility (Melbourne, Victoria, Australia). Library preparation was performed on isolated RNA samples using a TruSeq Stranded mRNA library preparation kit (Illumina), and sequencing was performed by obtaining 100-bp single reads.

RNAseq was performed for three donors, giving a total of 12 samples (i.e., three donors, influenza virus-exposed and -unexposed NK cells alone and total PBMCs), and a minimum of 2×10^7 reads/sample were generated. Differential gene expression profiling was performed between the three donors under two separate sets of conditions. RNAseq analysis was performed using the web-based Galaxy platform maintained by Melbourne Bioinformatics (50). Reads were mapped to the *Homo sapiens* reference genome (hg19) using the HISAT2 program (51), and reads were quantified using the HTSeq program (52). Differential counts were analyzed using the edgeR Bioconductor package (53). Pathway enrichment analysis was performed with a list of significantly upregulated genes ($P < 0.05$, log FC > 2) and visualized using the Enrichr tool (54).

Statistics. Statistical analysis was performed using Prism GraphPad (version 7) software (GraphPad Software, San Diego, CA). Samples were first assessed for the Gaussian distribution via the D'Agostino-Pearson omnibus normality test. The results presented in Fig. 1, 3, 5, and 7 to 9 were analyzed via one-way analysis of variance (ANOVA) with either Sidak's multiple-comparison test or Bonferroni's multiple-comparison *post hoc* tests. The parametric analysis whose results are shown in Fig. 5 was performed using separate Student *t* tests. The results in Fig. 11 were analyzed using a two-way ANOVA followed by Sidak's multiple-comparison test.

Accession number(s). Raw sequence reads can be accessed with GEO accession number GSE115203.

SUPPLEMENTAL MATERIAL

Supplemental material for this article may be found at https://doi.org/10.1128/JVI.02090-18.

SUPPLEMENTAL FILE 1, PDF file, 0.6 MB.

ACKNOWLEDGMENTS

This study was supported by funding from the Australian National Health and Medical Research Council.

We also thank Sarah Londrigan, Patrick Reading, Andrew Brooks, and Fernando Villalon for reagents and advice provided.

REFERENCES

1. Arnon TI, Achdout H, Lieberman N, Gazit R, Gonen-Gross T, Katz G, Bar-Ilan A, Bloushtain N, Lev M, Joseph A, Kedar E, Porgador A, Mandelboim O. 2004. The mechanisms controlling the recognition of tumor- and virus-infected cells by NKp46. Blood 103:664–672. https://doi.org/10.1182/blood-2003-05-1716.
2. Arnon TI, Lev M, Katz G, Chernobrov Y, Porgador A, Mandelboim O. 2001. Recognition of viral hemagglutinins by NKp44 but not by NKp30. Eur J Immunol 31:2680–2689. https://doi.org/10.1002/1521-4141(200109)31:9<2680::AID-IMMU2680>3.0.CO;2-A.
3. Gazit R, Gruda R, Elboim M, Arnon TI, Katz G, Achdout H, Hanna J, Qimron U, Landau G, Greenbaum E, Zakay-Rones Z, Porgador A, Mandelboim O. 2006. Lethal influenza infection in the absence of the natural killer cell receptor gene Ncr1. Nat Immunol 7:517–523. https://doi.org/10.1038/ni1322.
4. Mandelboim O, Lieberman N, Lev M, Paul L, Arnon TI, Bushkin Y, Davis DM, Strominger JL, Yewdell JW, Porgador A. 2001. Recognition of haemagglutinins on virus-infected cells by NKp46 activates lysis by human NK cells. Nature 409:1055–1060. https://doi.org/10.1038/35059110.
5. Bruhns P. 2012. Properties of mouse and human IgG receptors and their contribution to disease models. Blood 119:5640–5649. https://doi.org/10.1182/blood-2012-01-380121.
6. Perussia B, Acuto O, Terhorst C, Faust J, Lazarus R, Fanning V, Trinchieri G. 1983. Human natural killer cells analyzed by B73.1, a monoclonal antibody blocking Fc receptor functions. II. Studies of B73.1 antibody-antigen interaction on the lymphocyte membrane. J Immunol 130:2142–2148.
7. Ritz J, Schmidt RE, Michon J, Hercend T, Schlossman SF. 1988. Characterization of functional surface structures on human natural killer cells. Adv Immunol 42:181–211. https://doi.org/10.1016/S0065-2776(08)60845-7.
8. Bruhns P, Iannascoli B, England P, Mancardi DA, Fernandez N, Jorieux S, Daeron M. 2009. Specificity and affinity of human Fcgamma receptors and their polymorphic variants for human IgG subclasses. Blood 113:3716–3725. https://doi.org/10.1182/blood-2008-09-179754.
9. DiLillo DJ, Palese P, Wilson PC, Ravetch JV. 2016. Broadly neutralizing anti-influenza antibodies require Fc receptor engagement for in vivo protection. J Clin Invest 126:605–610. https://doi.org/10.1172/JCI84428.
10. DiLillo DJ, Tan GS, Palese P, Ravetch JV. 2014. Broadly neutralizing hemagglutinin stalk-specific antibodies require FcgammaR interactions for protection against influenza virus in vivo. Nat Med 20:143–151. https://doi.org/10.1038/nm.3443.
11. Impagliazzo A, Milder F, Kuipers H, Wagner MV, Zhu X, Hoffman RMB, van Meersbergen R, Huizingh J, Wanningen P, Verspuij J, de Man M, Ding Z, Apetri A, Kukrer B, Sneekes-Vriese E, Tomkiewicz D, Laursen NS, Lee PS, Zakrzewska A, Dekking L, Tolboom J, Tettero L, van Meerten S, Yu W, Koudstaal W, Goudsmit J, Ward AB, Meijberg W, Wilson IA, Rado Evi K. 2015. A stable trimeric influenza hemagglutinin stem as a broadly protective immunogen. Science 349:1301–1306. https://doi.org/10.1126/science.aac7263.
12. Henry Dunand CJ, Leon PE, Huang M, Choi A, Chromikova V, Ho IY, Tan GS, Cruz J, Hirsh A, Zheng NY, Mullarkey CE, Ennis FA, Terajima M, Treanor JJ, Topham DJ, Subbarao K, Palese P, Krammer F, Wilson PC. 2016. Both neutralizing and non-neutralizing human H7N9 influenza vaccine-induced monoclonal antibodies confer protection. Cell Host Microbe 19:800–813. https://doi.org/10.1016/j.chom.2016.05.014.
13. Yassine HM, Boyington JC, McTamney PM, Wei CJ, Kanekiyo M, Kong WP, Gallagher JR, Wang L, Zhang Y, Joyce MG, Lingwood D, Moin SM, Andersen H, Okuno Y, Rao SS, Harris AK, Kwong PD, Mascola JR, Nabel GJ, Graham BS. 2015. Hemagglutinin-stem nanoparticles generate heterosubtypic influenza protection. Nat Med 21:1065–1070. https://doi.org/10.1038/nm.3927.
14. Corti D, Voss J, Gamblin SJ, Codoni G, Macagno A, Jarrossay D, Vachieri SG, Pinna D, Minola A, Vanzetta F, Silacci C, Fernandez-Rodriguez BM, Agatic G, Bianchi S, Giacchetto-Sasselli I, Calder L, Sallusto F, Collins P, Haire LF, Temperton N, Langedijk JP, Skehel JJ, Lanzavecchia A. 2011. A neutralizing antibody selected from plasma cells that binds to group 1 and group 2 influenza A hemagglutinins. Science 333:850–856. https://doi.org/10.1126/science.1205669.
15. He W, Chen CJ, Mullarkey CE, Hamilton JR, Wong CK, Leon PE, Uccellini MB, Chromikova V, Henry C, Hoffman KW, Lim JK, Wilson PC, Miller MS, Krammer F, Palese P, Tan GS. 2017. Alveolar macrophages are critical for broadly-reactive antibody-mediated protection against influenza A virus in mice. Nat Commun 8:846. https://doi.org/10.1038/s41467-017-00928-3.
16. McBride JM, Lim JJ, Burgess T, Deng R, Derby MA, Maia M, Horn P, Siddiqui O, Sheinson D, Chen-Harris H, Newton EM, Fillos D, Nazzal D, Rosenberger CM, Ohlson MB, Lambkin-Williams R, Fathi H, Harris JM, Tavel JA. 2017. Phase 2 randomized trial of the safety and efficacy of MHAA4549A, a broadly neutralizing monoclonal antibody, in a human influenza A virus challenge model. Antimicrob Agents Chemother 61:e01154-17. https://doi.org/10.1128/AAC.01154-17.
17. Crowe JE, Jr. 2017. Principles of broad and potent antiviral human antibodies: insights for vaccine design. Cell Host Microbe 22:193–206. https://doi.org/10.1016/j.chom.2017.07.013.
18. Corti D, Cameroni E, Guarino B, Kallewaard NL, Zhu Q, Lanzavecchia A. 2017. Tackling influenza with broadly neutralizing antibodies. Curr Opin Virol 24:60–69. https://doi.org/10.1016/j.coviro.2017.03.002.
19. Jegaskanda S. 2018. The potential role of Fc-receptor functions in the development of a universal influenza vaccine. Vaccines (Basel) 6:E27. https://doi.org/10.3390/vaccines6020027.
20. Parsons MS, Richard J, Lee WS, Vanderven H, Grant MD, Finzi A, Kent SJ. 2016. NKG2D acts as a co-receptor for natural killer cell-mediated anti-HIV-1 antibody-dependent cellular cytotoxicity. AIDS Res Hum Retroviruses 32:1089–1096. https://doi.org/10.1089/aid.2016.0099.
21. Pegram HJ, Andrews DM, Smyth MJ, Darcy PK, Kershaw MH. 2011. Activating and inhibitory receptors of natural killer cells. Immunol Cell Biol 89:216–224. https://doi.org/10.1038/icb.2010.78.
22. Shields RL, Lai J, Keck R, O'Connell LY, Hong K, Meng YG, Weikert SH, Presta LG. 2002. Lack of fucose on human IgG1 N-linked oligosaccharide improves binding to human Fcgamma RIII and antibody-dependent cellular toxicity. J Biol Chem 277:26733–26740. https://doi.org/10.1074/jbc.M202069200.
23. Rajasekaran N, Chester C, Yonezawa A, Zhao X, Kohrt HE. 2015. Enhancement of antibody-dependent cell mediated cytotoxicity: a new era in cancer treatment. Immunotargets Ther 4:91–100. https://doi.org/10.2147/ITT.S61292.
24. Goodier MR, Rodriguez-Galan A, Lusa C, Nielsen CM, Darboe A, Moldoveanu AL, White MJ, Behrens R, Riley EM. 2016. Influenza vaccination generates cytokine-induced memory-like NK cells: impact of human cytomegalovirus infection. J Immunol 197:313–325. https://doi.org/10.4049/jimmunol.1502049.
25. Kuo RL, Zhao C, Malur M, Krug RM. 2010. Influenza A virus strains that circulate in humans differ in the ability of their NS1 proteins to block the activation of IRF3 and interferon-beta transcription. Virology 408:146–158. https://doi.org/10.1016/j.virol.2010.09.012.
26. Santoli D, Trinchieri G, Koprowski H. 1978. Cell-mediated cytotoxicity against virus-infected target cells in humans. II. Interferon induction and activation of natural killer cells. J Immunol 121:532–538.
27. Gerosa F, Gobbi A, Zorzi P, Burg S, Briere F, Carra G, Trinchieri G. 2005. The reciprocal interaction of NK cells with plasmacytoid or myeloid dendritic cells profoundly affects innate resistance functions. J Immunol 174:727–734. https://doi.org/10.4049/jimmunol.174.2.727.
28. Selva KJ, Kent SJ, Parsons MS. 2017. Modulation of innate and adaptive cellular immunity relevant to HIV-1 vaccine design by seminal plasma. AIDS 31:333–342. https://doi.org/10.1097/QAD.0000000000001319.
29. Diebold SS, Kaisho T, Hemmi H, Akira S, Reis e Sousa C. 2004. Innate antiviral responses by means of TLR7-mediated recognition of single-

stranded RNA. Science 303:1529–1531. https://doi.org/10.1126/science.1093616.
30. Le Goffic R, Pothlichet J, Vitour D, Fujita T, Meurs E, Chignard M, Si-Tahar M. 2007. Cutting edge: influenza A virus activates TLR3-dependent inflammatory and RIG-I-dependent antiviral responses in human lung epithelial cells. J Immunol 178:3368–3372. https://doi.org/10.4049/jimmunol.178.6.3368.
31. Pothlichet J, Meunier I, Davis BK, Ting JP, Skamene E, von Messling V, Vidal SM. 2013. Type I IFN triggers RIG-I/TLR3/NLRP3-dependent inflammasome activation in influenza A virus infected cells. PLoS Pathog 9:e1003256. https://doi.org/10.1371/journal.ppat.1003256.
32. Kato H, Sato S, Yoneyama M, Yamamoto M, Uematsu S, Matsui K, Tsujimura T, Takeda K, Fujita T, Takeuchi O, Akira S. 2005. Cell type-specific involvement of RIG-I in antiviral response. Immunity 23:19–28. https://doi.org/10.1016/j.immuni.2005.04.010.
33. Baum A, Garcia-Sastre A. 2010. Induction of type I interferon by RNA viruses: cellular receptors and their substrates. Amino Acids 38:1283–1299. https://doi.org/10.1007/s00726-009-0374-0.
34. Iwasaki A, Pillai PS. 2014. Innate immunity to influenza virus infection. Nat Rev Immunol 14:315–328. https://doi.org/10.1038/nri3665.
35. Adib-Conquy M, Scott-Algara D, Cavaillon JM, Souza-Fonseca-Guimaraes F. 2014. TLR-mediated activation of NK cells and their role in bacterial/viral immune responses in mammals. Immunol Cell Biol 92:256–262. https://doi.org/10.1038/icb.2013.99.
36. Hart OM, Athie-Morales V, O'Connor GM, Gardiner CM. 2005. TLR7/8-mediated activation of human NK cells results in accessory cell-dependent IFN-gamma production. J Immunol 175:1636–1642. https://doi.org/10.4049/jimmunol.175.3.1636.
37. Dreyfus C, Laursen NS, Kwaks T, Zuijdgeest D, Khayat R, Ekiert DC, Lee JH, Metlagel Z, Bujny MV, Jongeneelen M, van der Vlugt R, Lamrani M, Korse HJ, Geelen E, Sahin O, Sieuwerts M, Brakenhoff JP, Vogels R, Li OT, Poon LL, Peiris M, Koudstaal W, Ward AB, Wilson IA, Goudsmit J, Friesen RH. 2012. Highly conserved protective epitopes on influenza B viruses. Science 337:1343–1348. https://doi.org/10.1126/science.1222908.
38. Ekiert DC, Friesen RH, Bhabha G, Kwaks T, Jongeneelen M, Yu W, Ophorst C, Cox F, Korse HJ, Brandenburg B, Vogels R, Brakenhoff JP, Kompier R, Koldijk MH, Cornelissen LA, Poon LL, Peiris M, Koudstaal W, Wilson IA, Goudsmit J. 2011. A highly conserved neutralizing epitope on group 2 influenza A viruses. Science 333:843–850. https://doi.org/10.1126/science.1204839.
39. Ana-Sosa-Batiz F, Johnston APR, Hogarth PM, Wines BD, Barr I, Wheatley AK, Kent SJ. 2017. Antibody-dependent phagocytosis (ADP) responses following trivalent inactivated influenza vaccination of younger and older adults. Vaccine 35:6451–6458. https://doi.org/10.1016/j.vaccine.2017.09.062.
40. Ana-Sosa-Batiz F, Vanderven H, Jegaskanda S, Johnston A, Rockman S, Laurie K, Barr I, Reading P, Lichtfuss M, Kent SJ. 2016. Influenza-specific antibody-dependent phagocytosis. PLoS One 11:e0154461. https://doi.org/10.1371/journal.pone.0154461.
41. Jegaskanda S, Reading PC, Kent SJ. 2014. Influenza-specific antibody-dependent cellular cytotoxicity: toward a universal influenza vaccine. J Immunol 193:469–475. https://doi.org/10.4049/jimmunol.1400432.
42. He W, Tan GS, Mullarkey CE, Lee AJ, Lam MM, Krammer F, Henry C, Wilson PC, Ashkar AA, Palese P, Miller MS. 2016. Epitope specificity plays a critical role in regulating antibody-dependent cell-mediated cytotoxicity against influenza A virus. Proc Natl Acad Sci U S A 113:11931–11936. https://doi.org/10.1073/pnas.1609316113.
43. Leon PE, He W, Mullarkey CE, Bailey MJ, Miller MS, Krammer F, Palese P, Tan GS. 2016. Optimal activation of Fc-mediated effector functions by influenza virus hemagglutinin antibodies requires two points of contact. Proc Natl Acad Sci U S A 113:E5944–E5951. https://doi.org/10.1073/pnas.1613225113.
44. Stein-Streilein J, Guffee J. 1986. In vivo treatment of mice and hamsters with antibodies to asialo GM1 increases morbidity and mortality to pulmonary influenza infection. J Immunol 136:1435–1441.
45. Stein-Streilein J, Guffee J, Fan W. 1988. Locally and systemically derived natural killer cells participate in defense against intranasally inoculated influenza virus. Reg Immunol 1:100–105.
46. Zhou G, Juang SW, Kane KP. 2013. NK cells exacerbate the pathology of influenza virus infection in mice. Eur J Immunol 43:929–938. https://doi.org/10.1002/eji.201242620.
47. Abdul-Careem MF, Mian MF, Yue G, Gillgrass A, Chenoweth MJ, Barra NG, Chew MV, Chan T, Al-Garawi AA, Jordana M, Ashkar AA. 2012. Critical role of natural killer cells in lung immunopathology during influenza infection in mice. J Infect Dis 206:167–177. https://doi.org/10.1093/infdis/jis340.
48. World Health Organization. 2011. Manual for the laboratory diagnosis and virological surveillance of influenza. World Health Organization, Geneva, Switzerland.
49. Jegaskanda S, Job ER, Kramski M, Laurie K, Isitman G, de Rose R, Winnall WR, Stratov I, Brooks AG, Reading PC, Kent SJ. 2013. Cross-reactive influenza-specific antibody-dependent cellular cytotoxicity antibodies in the absence of neutralizing antibodies. J Immunol 190:1837–1848. https://doi.org/10.4049/jimmunol.1201574.
50. Afgan E, Sloggett C, Goonasekera N, Makunin I, Benson D, Crowe M, Gladman S, Kowsar Y, Pheasant M, Horst R, Lonie A. 2015. Genomics virtual laboratory: a practical bioinformatics workbench for the cloud. PLoS One 10:e0140829. https://doi.org/10.1371/journal.pone.0140829.
51. Kim D, Langmead B, Salzberg SL. 2015. HISAT: a fast spliced aligner with low memory requirements. Nat Methods 12:357–360. https://doi.org/10.1038/nmeth.3317.
52. Anders S, Pyl PT, Huber W. 2015. HTSeq—a Python framework to work with high-throughput sequencing data. Bioinformatics 31:166–169. https://doi.org/10.1093/bioinformatics/btu638.
53. Robinson MD, McCarthy DJ, Smyth GK. 2010. edgeR: a Bioconductor package for differential expression analysis of digital gene expression data. Bioinformatics 26:139–140. https://doi.org/10.1093/bioinformatics/btp616.
54. Chen EY, Tan CM, Kou Y, Duan Q, Wang Z, Meirelles GV, Clark NR, Ma'ayan A. 2013. Enrichr: interactive and collaborative HTML5 gene list enrichment analysis tool. BMC Bioinformatics 14:128. https://doi.org/10.1186/1471-2105-14-128.